

Pattern and morphogenesis of presumptive superficial mesoderm in two closely related species, *Xenopus laevis* and *Xenopus tropicalis*[☆]

David R. Shook,^{*} Christina Majer, and Ray Keller

Department of Biology, University of Virginia, Gilmer Hall, Charlottesville VA, 22903, USA

Received for publication 17 October 2003, revised 20 February 2004, accepted 20 February 2004

Available online 9 April 2004

Abstract

The mesoderm, comprising the tissues that come to lie entirely in the deep layer, originates in both the superficial epithelial and the deep mesenchymal layers of the early amphibian embryo. Here, we characterize the mechanisms by which the superficial component of the presumptive mesoderm ingresses into the underlying deep mesenchymal layer in *Xenopus tropicalis* and extend our previous findings for *Xenopus laevis*. Fate mapping the superficial epithelium of pregastrula stage embryos demonstrates ingression of surface cells into both paraxial and axial mesoderm (including hypochord), in similar patterns and amounts in both species. Superficial presumptive notochord lies medially, flanked by presumptive hypochord and both overlie the deep region of the presumptive notochord. These tissues are flanked laterally by superficial presumptive somitic mesoderm, the anterior tip of which also appears to overlay the presumptive deep notochord. Time-lapse recordings show that presumptive somitic and notochordal cells move out of the roof of the gastrocoel and into the deep region during neurulation, whereas hypochordal cells ingress after neurulation. Scanning electron microscopy at the stage and position where ingression occurs suggests that superficial presumptive somitic cells in *X. laevis* ingress into the deep region as bottle cells whereas those in *X. tropicalis* ingress by “relamination” (e.g., [Dev. Biol. 174 (1996) 92]). In both species, the superficially derived presumptive somitic cells come to lie in the medial region of the presumptive somites during neurulation. By the early tailbud stages, these cells lie at the horizontal myoseptum of the somites. The morphogenic pathway of these cells strongly resembles that of the primary slow muscle pioneer cells of the zebrafish. We present a revised fate map of *Xenopus*, and we discuss the conservation of superficial mesoderm within amphibians and across the chordates and its implications for the role of this tissue in patterning the mesoderm.

© 2004 Elsevier Inc. All rights reserved.

Keywords: Fate map; Adaxial cells; Primary slow muscle pioneer cells; Notochord; Somites; Hypochord; Epithelial to mesenchymal transition; Ingression; Surface mesoderm; *Xenopus laevis*; *Xenopus tropicalis*; Evolution of development; Variation in developmental mechanism; Gastrulation; Relamination; Bottle cells; Apical constriction

Introduction

Dramatic cellular rearrangements early in development bring the presumptive germ layers, arising as disparate cell populations within the embryo, into their definitive spatial relationships, with ectoderm lining the outer surface of the embryo, endoderm lining the inner (gut) surface, and mesoderm between the two. Much of this rearrangement

occurs during gastrulation, although in many vertebrates, it continues through neurulation and beyond.

Presumptive mesoderm originating in the superficial epithelial layer poses interesting problems as its morphogenesis is necessarily different from that of deep presumptive mesoderm. Presumptive mesoderm originating in the multi-layered deep region of the involuting marginal zone (IMZ, Fig. 1A), which has a mesenchymal organization, undergoes a relatively simple morphogenesis in that involution of the IMZ during gastrulation brings it into its definitive position between the endodermal lining of the archenteron (a definitive gut cavity, lined entirely by endoderm) and the overlying ectoderm (Fig. 1B). On the other hand, presumptive mesoderm originating in the superficial monolayer of the IMZ (Fig. 1C), which has an epithelial

[☆] Supplementary data associated with this article can be found, in the online version, at [doi:10.1016/j.ydbio.2004.02.021](https://doi.org/10.1016/j.ydbio.2004.02.021).

^{*} Corresponding author. Department of Biology, University of Virginia, Gilmer Hall, PO Box 400328, Charlottesville VA, 22904 4328. Fax: +1-434-982-5626.

E-mail address: drs6j@virginia.edu (D.R. Shook).

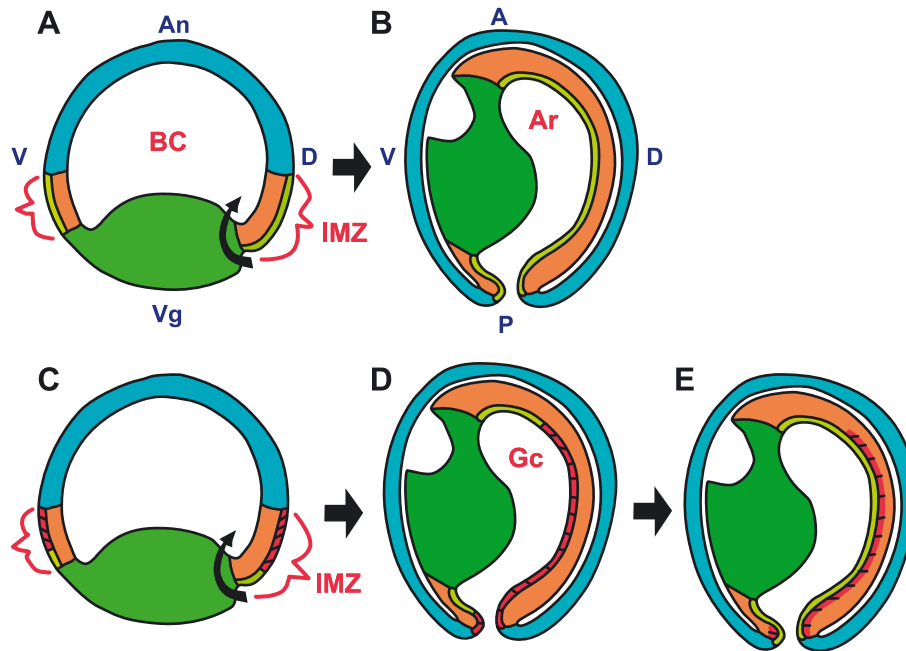


Fig. 1. Diagrams of hypothetical amphibian gastrulation movements (A, B) show that involution (curved arrow) of an involuting marginal zone (IMZ, brackets) with presumptive mesoderm only in the deep layer (pink) brings this germ layer into its definitive position between the ectoderm (blue) and the lining of the archenteron (Ar) or presumptive gut (yellow-green). (C, D) In contrast, the same morphogenic movement, involution (curved arrow), of an IMZ with presumptive mesoderm in the superficial epithelial layer (red-hatched) leaves this component of the presumptive mesoderm on the surface of the roof of the gastrocoel (Gc), necessitating its removal by an additional morphogenic movement, ingression, during neurulation (D, E). Blue: ectoderm; green: sub-blastoporal endoderm; yellow-green: supra-blastoporal endoderm; pink: deep mesoderm; red-hatched: mesoderm originating superficially. V: ventral; D: dorsal; An: animal; Vg: vegetal, A: anterior, P: posterior.

organization, remains on the topological surface of the embryo as the lining of the roof of the gastrocoel (a primitive gut cavity, not lined entirely by endoderm), after involution of the marginal zone (Fig. 1D). The superficial presumptive mesoderm must then move out of this layer and into the underlying deep mesenchymal layer (i.e., ingress) to differentiate into definitive mesoderm, leaving an archenteron lined entirely by endoderm (Fig. 1E). This ingress movement is part of an epithelial–mesenchymal transition (EMT) that these cells undergo (Shook and Keller, 2003).

Fate mapping studies show that by the end of neurulation in amphibians, including *Xenopus laevis*, superficial presumptive mesoderm has moved from the roof of the gastrocoel into the notochord and somites, as in Fig. 1E (Minsuk and Keller, 1996, 1997; Pasteels, 1942; Purcell and Keller, 1993; Vogt, 1929). The origin and morphogenesis of the hypochord has not been well characterized (Cleaver et al., 2000). As cells leave the surface layer, the medial margins of the lateral endodermal crests (LECs) (yellow green, Fig. 2B), which originate as the animal and medial edge of the supra-blastoporal endoderm (yellow green, Fig. 2A), move toward the dorsal midline, eventually fusing there. This process begins anteriorly and progresses toward the blastopore (Figs. 2C and D). Cells either ingress as individual bottle cells with constricted apices and elongated apical–basal axes (e.g., Purcell and Keller, 1993) (see Fig. 2E), or they relaminate as groups of cells that integrate their basal–lateral region into the underlying mesoderm before their

apices are covered by the LECs, and without any apparent constriction of the apices of the relaminated cells (e.g., Minsuk and Keller, 1996) (see Fig. 2F).

Keller (1975), based on vital dye marking experiments, concluded that in *X. laevis*, no mesoderm came from the superficial layer. A few marks applied to the superficial layer later appeared in the deep layer, but these were assumed to be marks that penetrated into the deep layer when they were made. Smith and Malacinski (1983), using Bolton-Hunter reagent, likewise concluded that the superficial layer made no “significant” contribution to the mesoderm, despite finding small patches of surface-labeled cells in the notochord in half of their 16 samples and in the adjacent somites in one of these. Minsuk and Keller (1997), using surface biotinylation and transplantation of fluorescent dextran-labeled epithelia, found labeled cells in the tailbud stage embryo, scattered throughout the notochord, and in the somites, just ventral to the horizontal myoseptum, in some, but not all of the *X. laevis* embryos they examined.

Here, we show that there is a significant superficial contribution to the mesoderm in *X. laevis* and in *Xenopus tropicalis*, a close diploid relative of the pseudo-tetraploid *X. laevis* (Cannatella and De Sa, 1993; De Sa and Hillis, 1990). We also characterize the extent, timing, pattern, and mechanism of mesoderm ingress in these species. Previous work suggested that *X. laevis* had either no or sporadic superficial mesoderm (Keller, 1976; Minsuk and Keller, 1997), whereas a species of the closest neighbor genus, *Hymenochirus* (De Sa

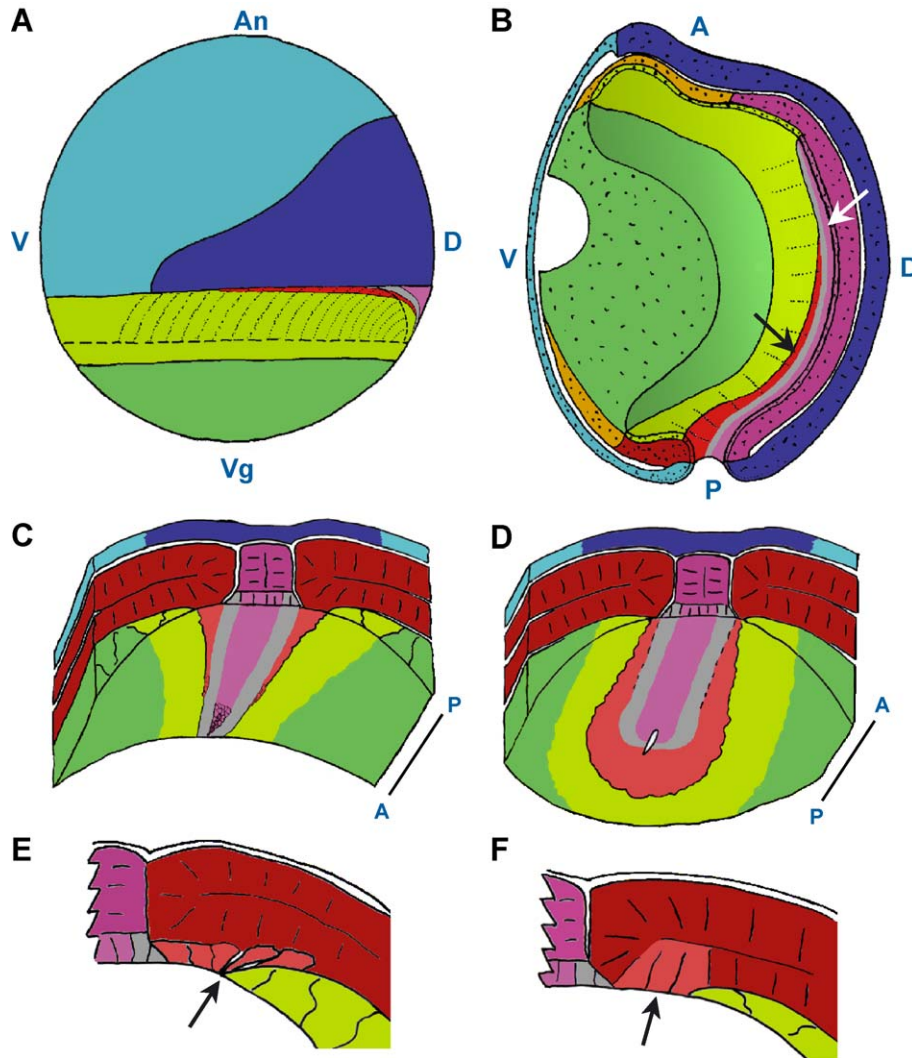


Fig. 2. Diagrams of superficial mesoderm morphogenesis. Bluish colors represent presumptive ectoderm (light blue: epidermis, dark blue: neural), reddish colors presumptive mesoderm (magenta: notochordal, red: somitic, orange: head, lateral and ventral mesoderm), greenish colors represent presumptive endoderm (yellow-green: supra-blastoporal endoderm, lime green: sub-blastoporal endoderm), gray represents presumptive hypochord. Dorsal (D), ventral (V), animal (An), vegetal (Vg), anterior (A), and posterior (P) are indicated. The stage 10 fate map (A) shows only the superficial view. In the ectodermal and vegetal endodermal regions above and below the IMZ, respectively, the presumptive fates continue radially toward the blastocoel. The surface of the IMZ is primarily covered by supra-blastoporal endoderm, with a smaller contribution from the superficial presumptive mesodermal tissues shown here is an approximation. Within the deep layer of the IMZ, presumptive head and lateral-ventral mesoderm lies vegetal of the horizontal dashed line, presumptive notochord lies dorsally of the vertical curved dashed line, and the presumptive somites are indicated by the dotted lines. A sagittal view of presumptive tissues near the end of gastrulation (stage 12.5) (B). Stippling indicates tissue that has been cut through, whereas the unstippled gastrocoel curves into the plane of the paper. The remaining yolk plug is not shown, to aid visualization of the gastrocoel roof plate. Presumptive notochordal (white arrow) and somitic cells (black arrow) are still in the superficial layer, with presumptive hypochordal cells between them; together, these form the gastrocoel roof plate. The medial edge of the supra-blastoporal endoderm forms the lateral endodermal crest. A transversely cut segment of the anterior gastrocoel roof (C), stage 15, showing the closure of the LECs at the midline anteriorly. A transversely cut segment of the posterior gastrocoel roof (D), including the slit blastopore, stage 15. Ingression of presumptive superficial somitic cells as bottle cells (E, arrow). Relamination of presumptive superficial somitic cells (F, arrow) onto the deep somitic tissue.

and Hillis, 1990), consistently had surface mesoderm, which moved into the deep layer by relamination, a mechanism never observed in *X. laevis* (Minsuk and Keller, 1996). We therefore expected *X. tropicalis* to be an interesting intermediate in the evolution of superficial mesoderm morphogenesis within the pipid amphibians.

All amphibians (Brauer, 1897; Delarue et al., 1992, 1994, 1995; Minsuk and Keller, 1996, 1997; Pasteels, 1942;

Purcell and Keller, 1993; Sarasin and Sarasin, 1887–1890; Shook et al., 2002; Smith and Malacinski, 1983; Vogt, 1929), and all other chordates studied (Balfour, 1885; Ballard, 1973, 1980; Conklin, 1905, 1932; Lawson et al., 1991; Nelsen, 1953; Nieuwkoop and Sutasurya, 1979; Psychoyos and Stern, 1996; Schoenwolf et al., 1992; Shih and Fraser, 1995) have at least some mesoderm in the pre-gastrula superficial epithelium. The ubiquity of superficial

presumptive mesoderm, even reduced to the minimal state found in *X. laevis*, suggests that this is a conserved ancestral character for amphibians and that it either has, or is closely associated with, an important functional role in amphibian development. We have taken a comparative approach to studying superficial mesodermal morphogenesis in *X. laevis* and *X. tropicalis* in the current paper, and in urodeles in a companion paper (Shook et al., 2002). We wish to determine exactly which morphogenic, and ultimately, which cell biological characters are conserved and which vary among species. This should allow us to understand which characters are relevant to the evolutionarily conserved function, which depend on species-specific conditions, and which characters show correlated changes, suggesting potential functional interactions.

Methods

Embryo culture

X. laevis embryos were obtained and cultured by standard methods (Kay and Peng, 1991). *X. tropicalis* embryos were obtained and cultured following the mating the protocol from the University of Virginia *X. tropicalis* Web site (<http://faculty.virginia.edu/xtropicalis/husbandry/TropmatingNew.htm>), except that they were raised in 1/6X MBS (Modified Barth's Saline). *X. laevis* and *X. tropicalis* were both staged according to Nieuwkoop and Faber (1967).

Embryo explants

Dorsal isolates, a modification of the "filets" of Minsuk and Keller (1996) or of Wilson explants (Wilson et al., 1989), were made at stages 12 to 13 and consisted of roughly the dorsal 180° of the embryo, from the blastopore through roughly 80% of the way to the anterior end of the gastrocoel. Dorsal isolates were allowed to heal 30 min to 1 h under a coverslip. We then observed the gastrocoel roof side of these explants, with coverslip removed or only lightly applied (see Time lapse microscopy below).

Giant sandwich explants (Keller et al., 1999; Poznanski and Keller, 1997; Poznanski et al., 1997) made here differed in that the blastoporal lip and presumptive bottle cells were included, plus sub-blastoporal endoderm extending 1–3 cells below the blastopore. Giant sandwich explants were allowed to heal under coverslip for 30 min to 1 h, then viewed without coverslip (see Time lapse microscopy below).

Biotinylation

Embryos were surface-labeled with biotin, usually just before gastrulation, based on the method of Minsuk and Keller (1997). Embryos were labeled with 1 mg/ml of EZ-link Sulfo-NHS-LC-biotin (Pierce no. 21335), made fresh

and pH adjusted to approximately 7.5. At the desired stage, embryos were fixed in MEMFA (Kay and Peng, 1991) overnight (O/N) at 4°C and then processed immediately or stored in methanol at –20°C.

Two methods were used for visualizing the distribution of biotin in fixed embryos. In the first, embryos were rehydrated, if necessary, then cleanly fractured in the desired orientation, using a no. 15 scalpel, in TBS + 0.1% tween-20 (TBtw). Embryo fragments were blocked in TBtw + 1% BSA for 3 h at room temperature, then incubated with rhodamine-conjugated avidin D (Vector no. A-2002) at 1:200 in TBtw + 1% BSA O/N at 4°C. Embryos were rinsed with TBtw 3× over the course of the next day, stored at –20°C in 100% methanol and viewed under confocal microscopy (see below). This method was most successful with albino embryos, as remaining pigment interferes with the confocal laser beam, decreasing signal strength and resolution. In the second method, embryos were embedded in paraffin and sectioned at 10 µm. The sections were rehydrated, bleached if necessary (see below), incubated with alkaline phosphatase-conjugated avidin or streptavidin, and then developed with NBT/BCIP (Promega, no. S380C and no. S381C) or Magenta-phosphate (Biosynth AG, no. B755). Slides were then dehydrated and mounted with Permount. Control, un-biotinylated embryos showed no signal on the addition of avidin-alkaline phosphatase and color reactants.

Bleaching embryos

Embryos with very strong pigment were bleached before or after the alkaline phosphatase reaction by leaving the slides overnight in buffered saline + 1% H₂O₂. Alternatively, bleaching of whole embryos or embryo explants or fragments was done in 0.5× SSC, 5% Formamide and 1% H₂O₂ for 1 to 4 h, under a fluorescent light (Mayor et al., 1995).

Fluorescent labeling and grafting of epithelial layers

Embryos were injected at the one or two cell stage to a final concentration of about 40 ng per µl of cell volume (e.g., 45 ng into a whole *X. laevis* embryo, 9 ng into a *X. tropicalis* embryo) of lysine-fixable rhodamine-dextran, 10 kDa (Molecular Probes D-1817) (RDA). Patches of the superficial epithelial layer from the IMZ were grafted homotopically at stages 10 to 10.25 from labeled embryos into unlabeled hosts, as described previously (Shih and Keller, 1992b). The position of grafts was either estimated by eye, or measured from a video image of the host embryo (see Image analysis and processing below). The medial and lateral edges of the transplant were measured in degrees from the midline, taking the center of the vegetal yolk mass as the origin. Embryos were fixed in MEMFA (Kay and Peng, 1991) at the early tailbud stage and sectioned for fluorescence microscopy as described previously (Keller

and Tibbetts, 1989). The presence of label in non-mesodermal tissues was used as a positive control. Negative controls are described within the text.

Confocal microscopy

Embryos were dehydrated in methanol, transferred to Murray clear (2:1 Benzyl Benzoate/Benzyl Alcohol) and observed with a Nikon PCM2000 laser scanning confocal coupled to TE-200 epifluorescence microscope.

Time lapse microscopy

Embryos and explants were recorded using a Dage MTI or Hamamatsu CCD video camera on a Zeiss SV6, or an Olympus SZH10 stereo microscope. Images were captured every 3 to 5 min. Images were transferred using a Scion image capture board and NIH image 1.6 software (Wayne Rasband, National Institutes of Health; available at <http://rsb.info.nih.gov/nih-image/>). Low-angle bright-field epillumination was used, and the lighting and cameras were adjusted to enhance the contrast between individual cells.

Image analysis and processing

Object Image 1.6, a modification of NIH image by Norbert Vischer (available at <http://simon.bio.uva.nl/object-image.html>) was used to track and make measurements of cell behavior and position in the time lapse recordings or still images. Three-dimensional projections of confocal image stacks were made using NIH Image 1.6.

Scanning electron microscopy

Embryos were fixed in 2.5% glutaraldehyde, 4% paraformaldehyde in 0.1M Phosphate buffer, pH 7.4 overnight, then postfixed in OsO₄. Samples were dehydrated through an ethanol series, critical point dried, mounted on blocks with silver paint, and then sputter coated. Specimens were then observed on a JEOL 6400, and images captured onto Polaroid film.

Results

Specificity of biotinylation

Surface biotinylation before the onset of gastrulation labeled the entire surface, and only the surface of the embryo through the end of gastrulation (e.g., Fig. 3A) and allowed us to follow the combined fates of all superficial cells throughout later development (see also Minsuk and Keller, 1997). During gastrulation and neurulation, concentrated, punctate biotin label was found internalized in cells with constricted apices, for example, in the blastoporal bottle cells (Fig. 3B), in the cells of the forming neural

tube (Figs. 3C, E), and in cells, in the gastrocoel roof of the neurula that appeared to be ingressing into the notochord (Figs. 3E, F, arrowheads) or pre-somitic mesoderm (Fig. 3D, arrowhead). Much of the label in ingressed pre-somitic and notochordal cells was inside the cells (Figs. 3E, F, arrows; Fig. 4B, e.g., in somitic cells indicated by arrows). Internalized biotin was also found in vegetal endoderm cells lining the walls and floor of the gastrocoel (Fig. 4A); these cells decrease their apical surface area before and during gastrulation (Keller, 1978). Observations of numerous vesicles in the apical ends of bottle cells in electron micrographs (see Baker, 1965; Balinsky, 1961; Lofberg, 1974; Perry and Waddington, 1966; Schroeder, 1970) suggest that biotin was internalized by endocytosis during apical constriction. Biotin label on cells that remain epithelial eventually finds its way into the basolateral membrane, as well as the cytoplasm, very slowly over time (e.g., Fig. 4A) (see also Muller and Hausen, 1995, their Fig. 7), such that by the end of gastrulation, biotin label was no longer confined to the apical membranes of the surface cells. It is not clear whether biotin is transcytosed to the basal–lateral membrane or whether it can drift across the apical–basal boundary at some low rate. More internalized and basolateral biotin was seen in cells that had undergone apical contraction, and hence increased endocytosis (e.g., compare neural and adjacent epithelial cells in Figs. 3C, E).

Biotin labeled deep vegetal endodermal cells were sometimes found at the late neurula stage (data not shown). These cells could have ingressed after being covered by the closing blastopore, since label was not generally found in the deep endoderm before the end of gastrulation (Fig. 4A), and time lapse filming showed no cells leaving the surface of the vegetal endoderm during gastrulation (Keller, 1978). Alternatively, endocytosis of biotin, followed by radial division (i.e., with the mitotic spindle oriented perpendicular to the surface) of superficial cells could account for labeled deep vegetal endoderm. With the exception of the deep vegetal endodermal cells, we are confident that labeled cells found in the deep layer after neurulation ingressed from the superficial layer, both because radial divisions from the epithelial layer end as gastrulation begins (Chalmers et al., 2003), and because biotin label in the deep layer is always restricted to specific positions within the mesoderm (see below).

Fate of superficial mesoderm

Similar mesodermal tissues were labeled in *X. laevis* and *X. tropicalis*. In both species, roughly 5% of the mid to posterior somitic mesoderm and roughly 20% of the notochord originated superficially, as estimated from the area labeled in sections (data not shown). Superficial presumptive mesodermal cells began moving into the deep layer and joining the notochordal or pre-somitic mesoderm during neurulation. This process began at about stage 13 in *X. tropicalis* and stage 15 in *X. laevis*, based on the earliest observation of deep label (data not shown).

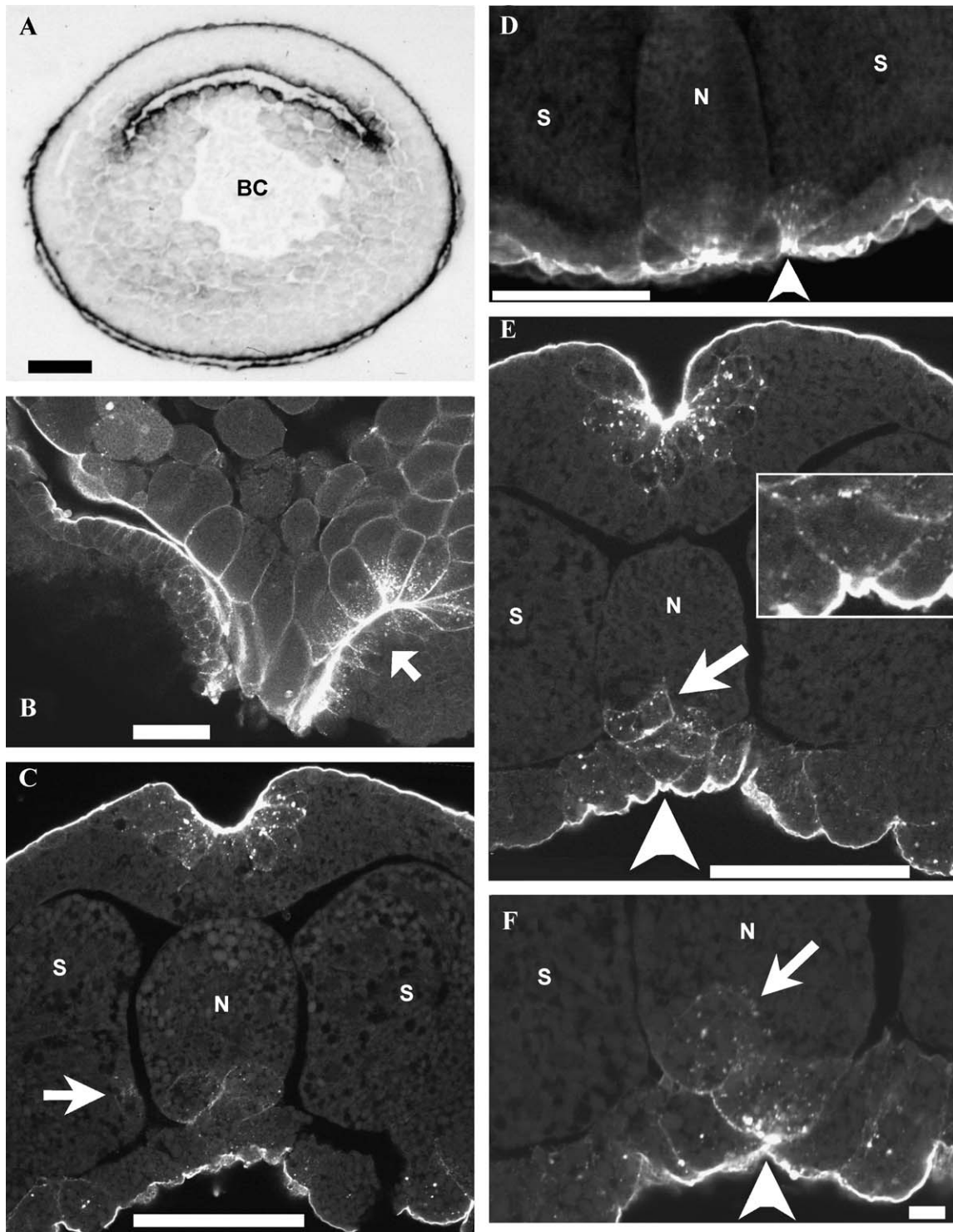


Fig. 3. At stage 12+ in *X. tropicalis*, before the onset of ingress, no biotin label is seen in the deep layers (A); BC = blastocoel remnant. In *X. laevis* at stage 12.5, a sagittal confocal section (B) shows a great deal of internalized biotin label in cells with recently constricted apices (cells lining the ventral portion of the gastrocoel, arrow). In *X. laevis* at stages 17–18, a transverse confocal section (C) through the mid-trunk region of an embryo raised at 15°C shows a faintly labeled ingressed pre-somatic (arrow) cell. Transverse confocal sections of stage 17–18 *X. laevis* embryos raised at room temperature (D–F). Inset in (E) is a higher magnification view of the ingressing cell indicated by the arrowhead. S = pre-somatic mesoderm, N = notochord. Embryo in (A) visualized via alk-phos avidin; embryos in (B–F) visualized via rhodamine avidin. Scale bars in A, B, C, D, E = 100 μm ; F = 10 μm .

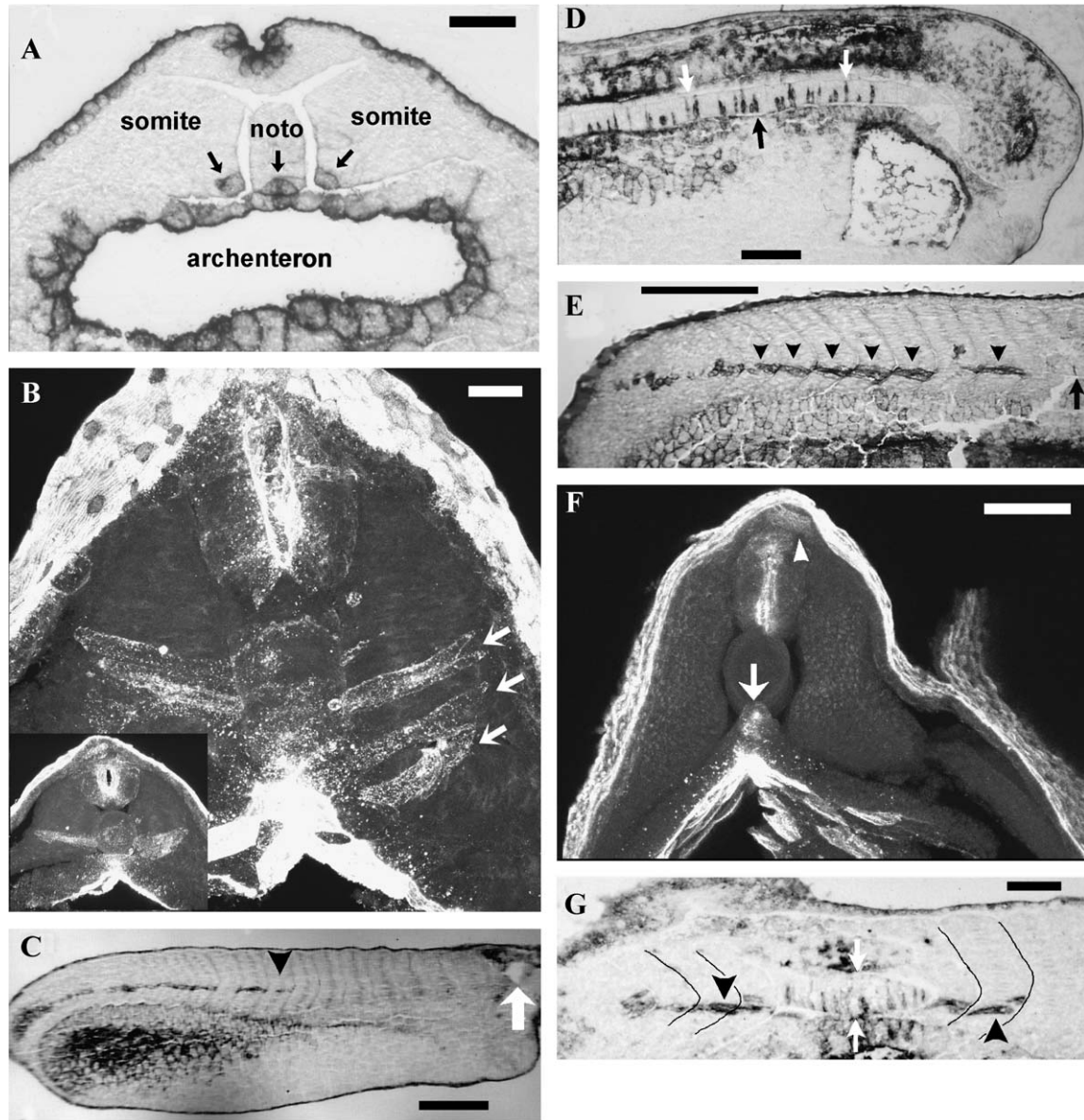


Fig. 4. Biotinylation of *Xenopus laevis* embryos before gastrulation shows the collective fates of the superficial layer. In *X. laevis* at stage 18, a transverse section (A) shows a single cell with biotin label in each somite, and two cells in the base of the notochord (arrows). In *X. laevis* at stages 22–23, a projection of a confocal series through the mid-posterior trunk of the embryo at about 45° off transverse (B) shows biotin-labeled somitic cells (arrows) project out from the notochord. Inset shows the projection rotated to transverse plane. (the projection can also be rotated: Fig. S1a at http://faculty.virginia.edu/shook/xen1/supp_figs.htm). In *X. laevis* at stage 26, an off-sagittal section (C) shows fairly continuous labeling through the mid-posterior somites, with the most anterior labeled somite (arrowhead) separated from the otic vesicle (arrow) by 7 or 8 unlabeled somites. In *X. laevis* at stage 26, a sagittal section (D) shows biotin label in the anterior notochord (delimited by black and white arrows). In *X. laevis* at stage 25, a sagittal section (E) shows two to three biotin-labeled somitic cells in each somite, just ventral of the horizontal myoseptum throughout most of the posterior trunk (arrowheads), even with the ventral base of the notochord (arrow); labeled cells are also evident in unsegmented tailbud presomitic mesoderm. In *X. laevis* at stages 24–25, a projection of transverse confocal series (F) shows no label in either the notochord or somites, but the neural tube is well labeled, as is the hypochord (arrow). A small patch of cells above the neural tube is also consistently labeled at this stage (arrowhead). In *X. laevis* at stages 25–26, a roughly sagittal section of a curved embryo (G) shows biotin labeled somitic cells just ventral of horizontal myoseptum (arrowheads), aligned with the base of the notochord (white arrows). Embryos in (A, C–E, and G) visualized via alk-phos avidin; embryos in (B and F) visualized via rhodamine avidin. Scale bar in B = 30 μm ; A, D, F, G = 100 μm ; C, E = 300 μm .

By mid-late neurula stages, biotin-labeled cells were found in the medial–ventral corners of the somites and in the ventral aspect of the notochord (Fig. 4A, arrows). Labeled cells were found only in these cross-sectional positions but not in every section along the anterior–posterior axis. By the tailbud stages, the labeled superfi-

cial cells that ingress into the notochord had intercalated radially with the unlabeled deep cells (Fig. 4D, arrows).

Shortly after neurulation, the lateral ends of the deep somitic cells of superficial origin extended across the entire width of the somitic mesoderm, toward the presumptive

epidermis, while maintaining contact with the notochord (Fig. 4B and inset). In this confocal series, the labeled cells appeared in clusters of 1 to 3, at intervals of roughly 36 ± 6 μm . No obvious correspondence was seen between the anterior–posterior positions of the labeled cells in the presomitic mesoderm and those in the notochord. During segmentation, the somites rotate such that their medial edge moves anteriorly and their lateral edge posteriorly, beginning anteriorly near the end of neurulation and progressing posteriorly (Hamilton, 1969; Youn and Malacinski, 1981) (reviewed in Keller et al., 2000). At this time, the surface-labeled cells reoriented their long axis from medial–lateral to anterior–posterior (Figs. 4C, E, G). One to three of these superficial cells came to lie at the horizontal myoseptum of each somite (Figs. 4E, G, arrowheads), at the level of the ventral part of the notochord (Figs. 4E, G, arrows). Biotin-labeled cells were generally absent in the anterior somites at the early tailbud stage (Fig. 4C). No biotin label was found in the 5 anterior trunk (post otic) somites (0/15 cases examined), suggesting that the anterior presumptive somites initially in contact with the notochord (Fig. 2A) have no superficial component (see Discussion). Labeled deep cells were always found posterior of the last morphologically distinct somite (e.g., Figs. 4C, E, and data not shown) in embryos in which notochordal and somitic labeling was evident, suggesting that the superficial contribution to notochord and the horizontal myoseptum of the somites extends into the tail region.

Biotin label was also often found in small groups of cells on the dorsal side of the neural tube (e.g., Fig. 4F, arrowhead), a position expected for neural crest cells. This suggests that some neural crest cells may be of superficial origin, perhaps from among the population of superficial cells that express *Xsna* (Linker et al., 2000).

As in Minsuk and Keller (1997), we found that some *X. laevis* embryos, especially those grown at lower temperatures (15–18°C), showed no biotin in the mesodermal layers by early tailbud stages (23–25), despite having clearly labeled neural tubes and epidermal layers and sometimes hypochords (e.g., Fig. 4F, arrow). Absence of biotin-labeled somitic and/or notochordal cells in some embryos may reflect real developmental variation in the presence of superficial presumptive mesoderm in *X. laevis* but we could not rule out the possibility that the biotin was endocytosed during ingression and then eliminated from the cell. Frequent observation of embryos with signal in the notochord and/or somites that was at the limits of detection (e.g., Fig. 3C, arrow) supported the idea that all embryos have surface mesoderm but different rates of endocytosis and degradation. Ingressed cells, which seem prone to endocytosing much of their apical membrane-bound biotin, would degrade more of their biotin, than, for example, neural cells, which retain heavy apical labeling (Figs. 4B, F; see also confocal sections in Fig. S1B at http://faculty.virginia.edu/shook/xen1/supp_figs.htm). If this is the case, we cannot rule out the possibility of superficial contribu-

tions to other mesodermal tissues than those we have documented. However, we have never observed any other tissues to be specifically labeled, arguing against this possibility.

Morphology of the gastrocoel roof plate

The gastrocoel roof plate is the population of presumptive mesodermal cells in the superficial epithelial layer of the gastrocoel roof. The regional organization of the gastrocoel roof was clearest in scanning electron micrographs of *X. tropicalis* at early–mid neurulation (Figs. 5A, B). The smaller cells of the gastrocoel roof plate (i.e., immediately superficial to the notochord and the medial edges of the somites, Fig. 5C) are flanked by the larger cells of the LECs (Figs. 5A, B arrowheads; Fig. 5C, arrows).

The anterior-to-posterior progression of gastrocoel roof plate closure in *X. tropicalis* was evident in the early neurula (Figs. 5A, B). Anteriorly, the presumptive notochordal and somitic mesoderm had ingressed by this stage, leaving only hypochord at the midline as far posteriorly as the mid-trunk level. The gastrocoel roof plate flared outward posterior from this point (Fig. 5A), and was broadest around the blastopore (Fig. 5B). Just posterior of the point of fracture, a few smaller presumptive notochordal cells remained at the midline, flanked only by hypochord (Fig. 5A, arrow). Two “zones” of the gastrocoel roof plate (Purcell and Keller, 1993) could be distinguished (Fig. 5A; see also Figs. 2C, D). Zone I is beneath the notochord and zone II is beneath the somites, on either side of zone I, separated from it by an obvious cellular boundary (Fig. 5A), which is continuous with that between the deep notochord and somites (see Figs. 6C and D). These zones continued around the lateral sides of the blastopore (Fig. 5B), which Purcell and Keller (1993) designated separately as zone III.

The organization of the mid-neurula stage *X. laevis* gastrocoel roof plate was similar, with a narrow gastrocoel roof plate anteriorly, flaring posteriorly (data not shown). However, the distinction between the LECs and the mesodermal gastrocoel roof plate was less obvious, and the boundary between zones I and II was not obvious in *X. laevis* (Fig. 5C).

Both in *X. laevis* and *X. tropicalis*, each cell in the gastrocoel roof plate but not the adjacent LEC cells, had one cilium growing out of its posterior edge (Figs. 5C, D, E, arrowheads; data not shown for *X. tropicalis*).

Variations in the mechanism of somitic mesoderm removal from the superficial layer

Superficial somitic cells in *X. laevis* ingressed into the deep layer as bottle cells, with constricted apical surfaces and apical–basal elongation (Figs. 6A, B; see also Fig. 2E). Cells near the medial–ventral corner of the somite, where biotin-labeled cells are commonly observed, typically

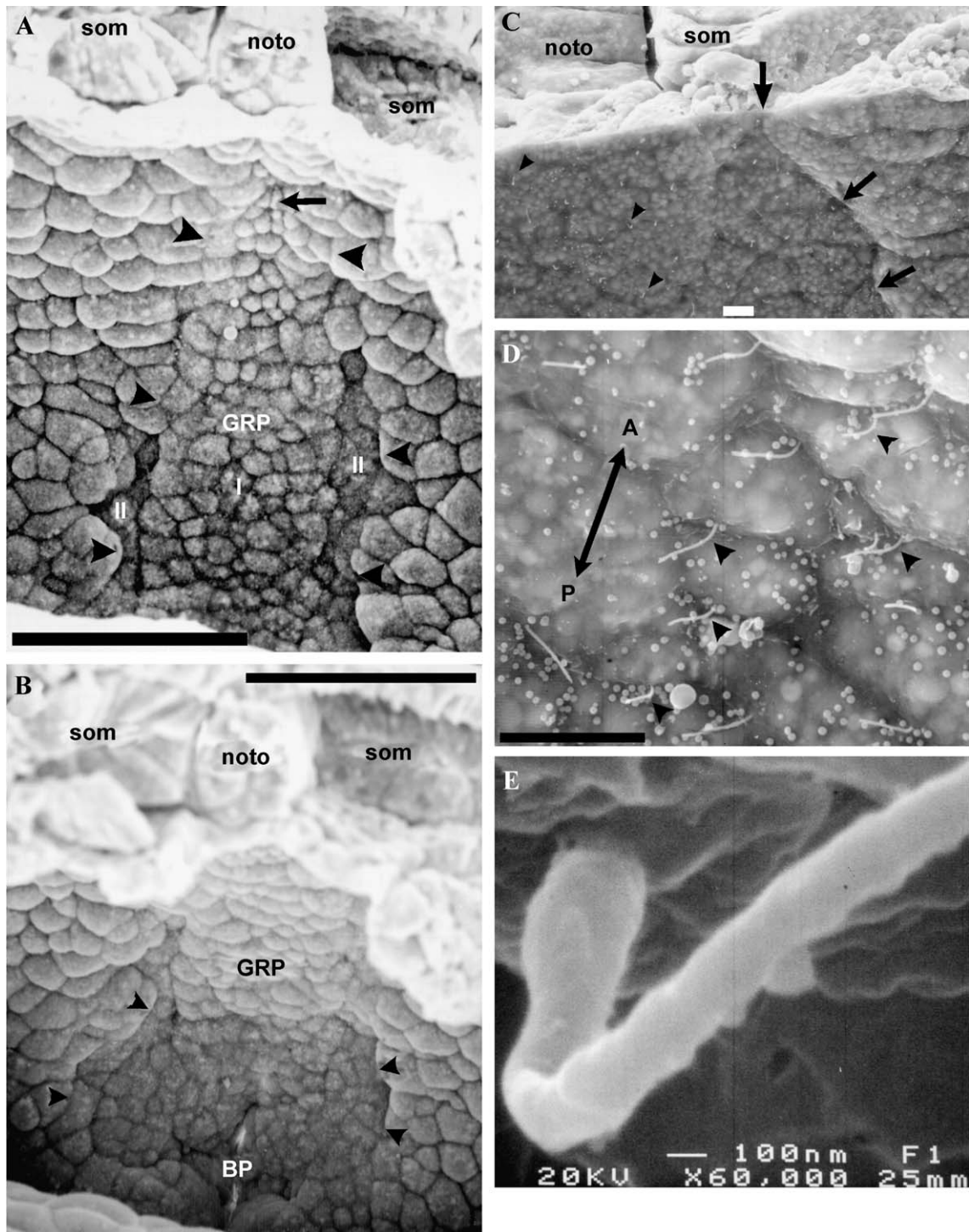


Fig. 5. SEM of gastrocoel roof plate. The posterior half of a transversely fractured stage 14 *X. tropicalis* embryo (A, B), with notochord (noto) and somites (som) indicated at the fractured face. The limits of the gastrocoel roof plate (GRP) are indicated (arrowheads). At the anterior end of the gastrocoel roof plate (A), notochordal cells with small apices (arrow) are flanked by hypochordal, and more laterally, endodermal cells, just posterior of the point of LEC fusion, which is at about the level of the fracture. Just posterior, the gastrocoel roof plate (GRP) becomes more distinct from the LECs, and two zones (I and II) are evident; zone I composes the superficial presumptive notochordal cells, flanked by the presumptive hypochordal cells. Zone II composes the superficial presumptive somitic cells. The posterior gastrocoel roof plate (B), with a slit blastopore (BP). SEM of cilia (C–E) (arrowheads) on the gastrocoel roof plate. A transverse fracture across gastrocoel roof plate (C), bounded by LEC (arrows). Anterior is up. Each cell in the gastrocoel roof plate has on its surface a single cilium (D). The A–P axis is indicated by double headed arrow. A cilium at high magnification (E). Scale bars in A, B = 100 μm ; C, D = 10 μm .

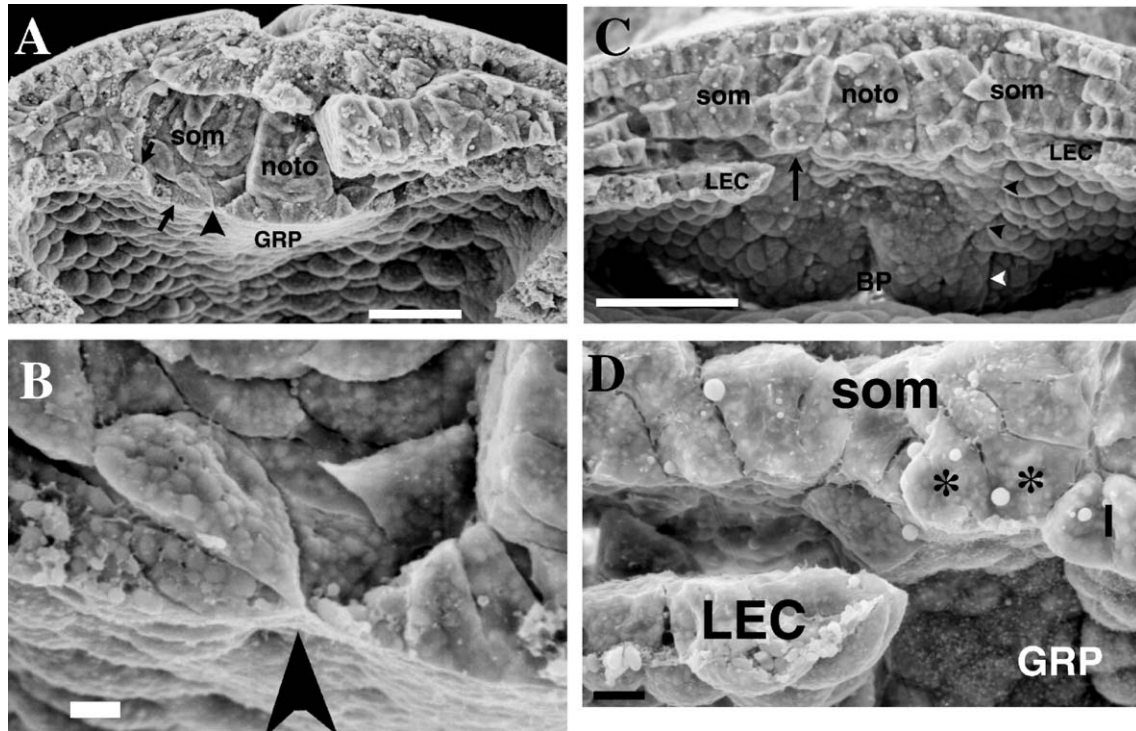


Fig. 6. SEMs showing the region of ingression. In *X. laevis* at stages 16–17, a transverse fracture through the mid-posterior trunk (A and B) shows a bottle-shaped cell ingressing into the medial–ventral corner of the left somite (A, B, arrow head) at the left edge of the gastrocoel roof plate (GRP); the LEC is also indicated (A, arrows). A close-up of the bottle cell (B, arrowhead), shows its apex still attached to the epithelial layer of the gastrocoel. In *X. tropicalis* at stages 14–16, a transverse fracture through the posterior trunk (C and D) shows superficial cells relaminating onto the underlying somitic tissue. The left LEC has fractured away from the underlying somite slightly, also breaking its normal lateral attachment to the gastrocoel roof plate (GRP). An overview shows two cells (C, arrow) just medial of the attachment point of the LEC that are both clearly part of the epithelial layer of the gastrocoel yet also clearly integrated into the somite above. A higher magnification shot (D) shows that neither cell (*s) has a bottle cell shape, or a particularly constricted apex. The right side of the gastrocoel roof plate is indicated (D, arrowheads). (I = edge of zone I). Scale bars in A, C = 100 μm ; B, D = 10 μm .

showed highly constricted apices while still integrated into the gastrocoel roof epithelium (Figs. 6A, B, arrowhead; see also Fig. 3D, arrowhead). Their basal ends lie lateral to the apical ends and bear a few small protrusions, suggesting that the apical end was pushed medially after the basal end began interacting with the deep cells. In contrast, superficial somitic cells in *X. tropicalis* moved into the deep layer by relamination (Figs. 6C, D; see also Fig. 2F). The basolateral ends of the relaminating cells integrated into the structure of the underlying mesodermal tissue, without leaving the epithelial layer, and their apices were subsequently covered by movement of the LECs medially. Apical constriction did not commonly occur and the apices were not displaced medially with respect to the basal ends (Figs. 6C, D).

Timing and pattern of ingression and relamination

Biotinylation shows the fate of the surface mesoderm, and SEM suggests the mechanism and pattern of ingression, but these static methods provide only snapshots of the morphogenic process. Time lapse video microscopy of the gastrocoel roof surface of dorsal isolate explants shows the dynamic pattern and timing of surface mesoderm ingression.

Our assumptions about cellular mechanics and its relation to apical behavior in time lapse movies should be made explicit. The apical surface is reduced in each case as cells ingress but whereas cells ingressing as bottle cells clearly concentrate their pigment in a contracting apex, relaminated presumptive somitic cells in *X. tropicalis* that are subsequently covered by the LECs generally do not concentrate pigment, presumably because their apical membrane is being covered, rather than decreasing in area (see below). In the case of cells that do concentrate apical pigment as they ingress, it is not clear whether pigment concentration indicates only active, for example, actin-myosin based apical contraction by the ingressing cells, or passive decrease in apical area, either by active pushing by neighboring cells, or removal of structures supporting the extent of the apical domain by the ingressing cell.

In *X. laevis*, the larger cells of the LECs (Fig. 7) moved medially as the smaller presumptive mesodermal cells in the gastrocoel roof plate constricted their apices and ingressed from the superficial layer (Fig. 7; see movie: Fig. S2 at http://faculty.virginia.edu/shook/xen1/supp_figs.htm). Closure of the LECs, especially over the posterior gastrocoel roof plate, was strongly progressive from anterior to posterior, such that by mid-neurula stage, the LECs were only

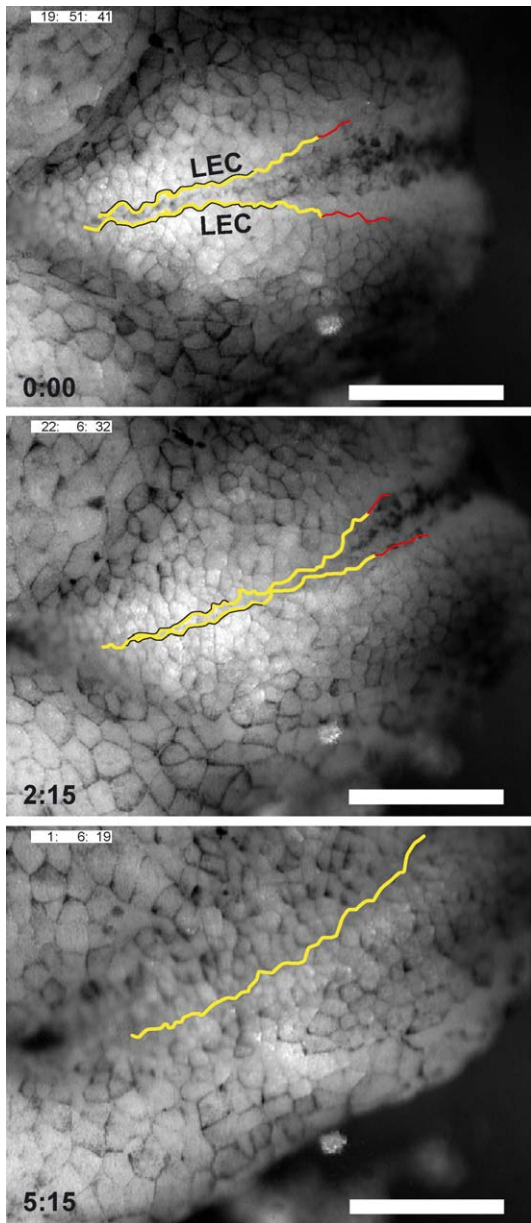


Fig. 7. Stills from a time-lapse movie of the closure of the gastrocoel roof plate in *X. laevis* at stages 16–17 (0:00), stage 19 (2:15), and stage 22 (5:15). The yellow lines indicate the medial margins of the LEC cells bordering those that ingress. Times below each frame indicate elapsed time from the first frame shown in hours:minute. An animated version of the movie is also available (Fig. S2, at http://faculty.virginia.edu/shook/xen1/supp_figs.htm). Scale bars = 300 μ m.

separated by the strip of remaining hypochord anteriorly while, posteriorly they were still moving over the presumptive mesoderm (Fig. 7, 0:00). Ingression into the presumptive mesoderm began at the lateral edge and progressed medially whereas ingression into the notochord only occurred medially (see also Figs. 3D, E, F, arrowheads). Most but not all of the cells in zone II, adjacent to the LECs, concentrated their pigment, indicating that they constricted their apices, before being covered by the LECs. Presumptive notochord cells at the midline also constricted their apices,

as indicated by concentrated pigment, beginning at least as early as the presumptive somitic cells.

In *X. tropicalis*, similar gross movements occurred, but the presumptive somitic cells adjacent to the medially converging LECs rarely constricted their apices before being covered, judging by the lack of cells that showed uniform apical constriction to produce a concentrated pigment spot (see Fig. S3a at http://faculty.virginia.edu/shook/xen1/supp_figs.htm). A few cells at the midline, however, did have concentrated pigment spots, indicating apical constriction. In higher-resolution movies, the medial–lateral dimension of the apices of the presumptive somitic cells was first reduced, until they were long and skinny, whereupon they rapidly decreased their length from posterior to anterior (data not shown), suggesting that the apices of these cells are covered, rather than constricting. In some instances, it appeared that protrusions spanned over the superficial presumptive somitic cells from LEC cells to presumptive hypochord cells.

In both species, the ingression of presumptive notochord and somite along most of the length of the trunk (excepting the most caudal region) was completed by control stage 19 (Fig. 7, 2:15) when the neural folds were also meeting. At this point, time lapse movies of both *X. laevis* and *X. tropicalis* showed that the remaining midline cells, the presumptive hypochord, began to ingress such that the LECs met at the midline along the entire A–P axis by about stage 22 in both *X. laevis* (Fig. 7, 5:15) and *X. tropicalis* (see Fig. S3 at http://faculty.virginia.edu/shook/xen1/supp_figs.htm) leaving the archenteron lined entirely by endoderm.

Location of the presumptive mesodermal cells in the superficial layer

Our biotinylation experiments showed that cells were ingressing from the superficial layer into mesodermal tissues but say nothing about their original organization within the superficial layer. To address this question, we made a series of homotopic epithelial transplants, from donor embryos labeled with rhodamine dextran into unlabeled hosts from which the homotopic epithelium had been removed (Fig. 8). These were examined at stage 26, by which time cells had finished ingressing and the last of these tissues, the hypochord, was morphologically distinct. Grafts made across the dorsal midline (e.g., Fig. 8A, -10° to $+10^\circ$) are useful for defining medial end points of superficial presumptive mesodermal tissues, whereas grafts made in the lateral marginal zone (e.g., Fig. 8A, $50^\circ+$) are useful for defining lateral end points. Initially, endpoints of each tissue were roughly defined by a series of transplants in which the lateral or medial edge of the transplant was estimated by eye. In later transplants, host embryos were imaged after excising an epithelial patch, to more accurately measure the edge of the transplant (e.g., Figs. 8B, D). Several examples of sections resulting from transplants to various locations

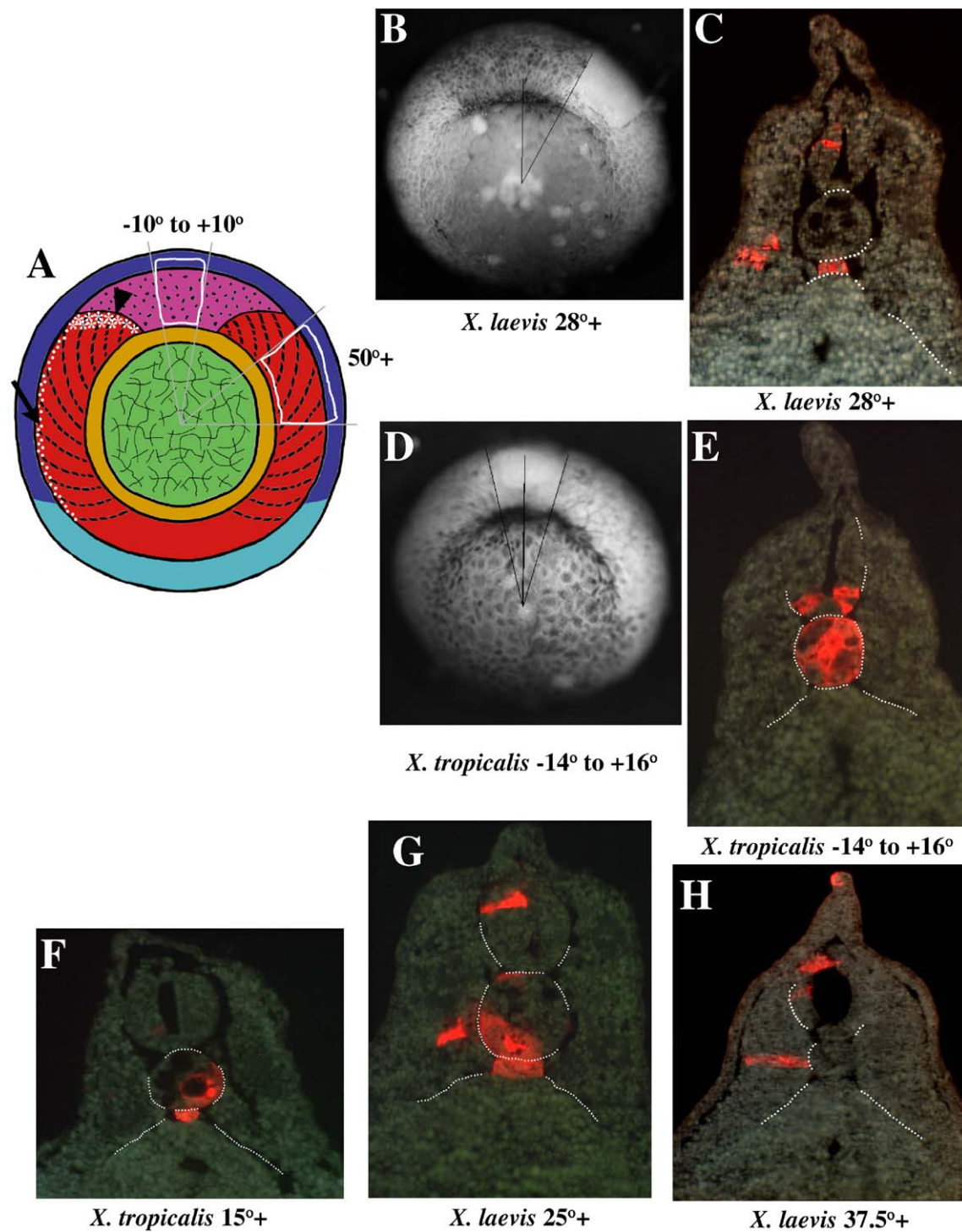


Fig. 8. Fluorescently labeled patches of superficial IMZ were transplanted homotopically at stage 10, and embryos were fixed at stage 26. A diagram of the stage 10 fate map of the deep region (A), viewed from the vegetal pole. Colors are as for Fig. 2. Superficial tissues are not shown around the IMZ in (A), but alternative initial locations of the superficial presumptive mesoderm are indicated depending on whether they shear with respect to the deep presumptive somites (*s), or the superficial presumptive notochord (white dots). Superficial epithelial tissue was excised from unlabeled host embryos, as shown in B and D, and graft locations were measured with respect to the midline; for example, in (A), one graft site (white outline) is shown spanning 10° on either side of the midline, and another is shown beginning 50° from the midline. In some cases, the operated host embryos were imaged and the location of the graft site measured on the image; in (B), the graft site began 28° from the midline, whereas in (D), the graft spanned from 14° on one side of the midline to 16° on the other side. (C) One section showing label from the graft made into the host embryo shown in (B); label is seen in both hypochordal and somitic tissues (as well as neural). (E) A section from the graft made into the host in (D); label is seen in notochord. Three more examples (F–H) from grafts made into the indicated locations, showing label in notochord and hypochord (F), notochord, hypochord and somite (G) or somite only (H). In C and E–H, morphological tissue boundaries are highlighted by a dotted white line.

show different contributions to the mesodermal tissues (Figs. 8C, E–H). For each transplant, the entire embryo was examined and the distribution of fluorescent label in each mesodermal tissue was recorded (Fig. 9). For *X. laevis*, the results from 66 transplants are shown (Fig. 9A), and for *X. tropicalis*, the results from 51 transplants are shown (Fig. 9B). Based on the earliest incidence of notochord, hypochord or somitic label in embryos with grafts that would be expected to include the most medial portion of the tissue in question, including some that were sectioned sagittally, it appears that superficial presumptive notochord contributes to the entire anterior–posterior length of the notochord, but there were no contributions of superficial cells to the first two trunk somites of the embryos (0/24 embryos examined), and infrequent contributions to the next two somites (4/24 embryos examined). As no biotin label was found in the first five trunk somites in biotinylated embryos (see above), fluorescently labeled cells contributing to the second pair of somites may have artifactually ingressed. Fluorescently labeled epithelial grafts covering the entire presumptive hypochordal region resulted in a hypochord with no unlabeled cells, indicating that its origin is entirely superficial.

There were several potential sources of error in the interpretation of the grafting data. First, we estimate that the endpoints of the transplant had accuracy's ranging from $\pm 10^\circ$ to $\pm 15^\circ$ for each of the “by eye” cases, and from $\pm 3^\circ$ to $\pm 5^\circ$ for each of the grafts measured from an image. This is due to possible mis-judgement of the center of the dorsal blastopore, or of the center of the yolk mass, and to the rapid deformation of the fate map between stages 10 and 10+, during the onset of gastrulation. Second, the center of the dorsal blastopore does not always perfectly predict the dorsal midline of the embryo but this is probably a fairly small component of error. Third, there may actually be some variation from embryo to embryo as to exactly how these tissues are patterned, particularly in *X. laevis*. Fourth, independent of variations in patterning, the path that any particular cell takes during morphogenesis is variable (e.g., Elul et al., 1997; Shih and Keller, 1992a) because of differences in cell cleavage orientation and cell rearrangements, rendering all fate maps statistical approximations (Keller, 1975, 1976). More dramatic examples of this type of variation are seen in fate maps made at the 32-cell stage in *X. laevis* (Bauer et al., 1994; Dale and Slack, 1987; Vodicka and Gerhart, 1995) or in the blastula stage zebrafish embryo (Kimmel et al., 1990). This source of variation may be ameliorated to some degree if epithelial cells rearrange less than mesenchymal cells. Fifth, the surgery may have altered the patterning of the superficial layer, for example, the graft may have healed poorly, or part of it may have died, such that it contributed to only one side of the transplant position. Sixth, there are potential problems with the interpretation of the position of the label. Labeled cells could reach the deep layer by three mechanisms. Cells could ingress during neurulation but not before, as is the endogenous situation. Deep cells could be transplanted with the transplanted epithelium, despite every effort to remove

them. Or epithelial cells could artifactually ingress before neurulation, for example, as a result of some complication of surgery. Control embryos that were biotinylated before surgery and fixed shortly after the rhodamine-labeled graft had healed in showed a low rate (about 10%) of rhodamine-labeled deep cells, primarily from more lateral grafts. In most instances, these cells also showed biotin label, indicating artifactual ingression, rather than transplanted deep cells. Thus, some of our positive results may be the result of artifactual ingression. However, only rhodamine-labeled cells that were found in positions in the somites stereotypically occupied by biotin-labeled cells in un-operated embryos were counted as positive, probably eliminating most of the artifactually ingressing cells. Rhodamine label found within the somites that were outside of these positions were generally limited to one or two cells, usually in the more lateral portion of the somite. In cases where it was not possible to be sure that the label was not in a stereotypical position, the label was counted as ambiguous (Figs. 9A, B, green points in the Somite graph). Finally, in some instances, it was difficult to tell whether a labeled cell was in fact in the hypochord proper, or in a cell just below the hypochord, due to incomplete differentiation or poor histology. These cells were also indicated as ambiguous (Figs. 9A, B, green points in the Hypochord graph). However, the general consistency of negative results for the lateral end of the presumptive notochord and hypochord, and the medial limit of the presumptive somite suggests that the data are reasonably reliable. We are less certain about the lateral limit of the superficial presumptive somite.

Thus, we wish to make it clear that the Superficial Marginal Zone Fates shown for each species (Figs. 9A, B) are approximations. It was not technically feasible to reliably make transplants that spanned less than 10° across the midline, so we do not know whether the notochord or hypochord span the midline; we have assumed that the notochord does span the midline, and that the hypochord does not, but has a medial limit somewhere inside 10° . The number of ambiguous cases for the lateral limit of the somite makes its endpoint uncertain, although it does appear to end somewhere beyond 90° but before 120° . Our grafting experiments did not test the animal-vegetal extent of each tissue; thus the boundaries in Fig. 9 are approximations based entirely on our observations of explants (see below). In addition, prior results suggest that there may be significant shear between the deep and superficial layers (Vodicka and Gerhart, 1995), such that the deep layer of the IMZ extends further anteriorly than the superficial layer; this is not reflected in our fate map. The results of the grafting experiments alone do not indicate whether the posterior portion of the presumptive hypochord lies in between the superficial presumptive notochord and somite, or between the somite and the supra-blastoporal endoderm; however, results from time lapse recordings of these regions in explants indicates the former situation (see below). Overall, the results were fairly similar for the two species, showing no significant differences.

The results of these experiments and the corresponding fate maps (Fig. 9) are corroborated by time lapse recordings of dorsal isolates (see Figs. S2 and S3 at http://faculty.virginia.edu/shook/xen1/supp_figs.htm) and giant sandwich explants (data not shown). Both show morphologically distinguishable superficial tissues (see also Figs. 3D; 5A, zones I and II; 6D; Fig. 7, 0:00) ingressing at different times and retromapping to locations approximating those in our

fate maps (Fig. 9). The most medial cells of zone I and the most lateral zone II cells ingress first, during neurulation, followed after neurulation by those in between (the more lateral cells of zone I, now medially located). As we know that the notochordal and somitic cells have finished ingressing by the end of neurulation, except in the tail region, whereas hypochord ingress is just beginning (data not shown, and see Cleaver et al., 2000), this later group of cells

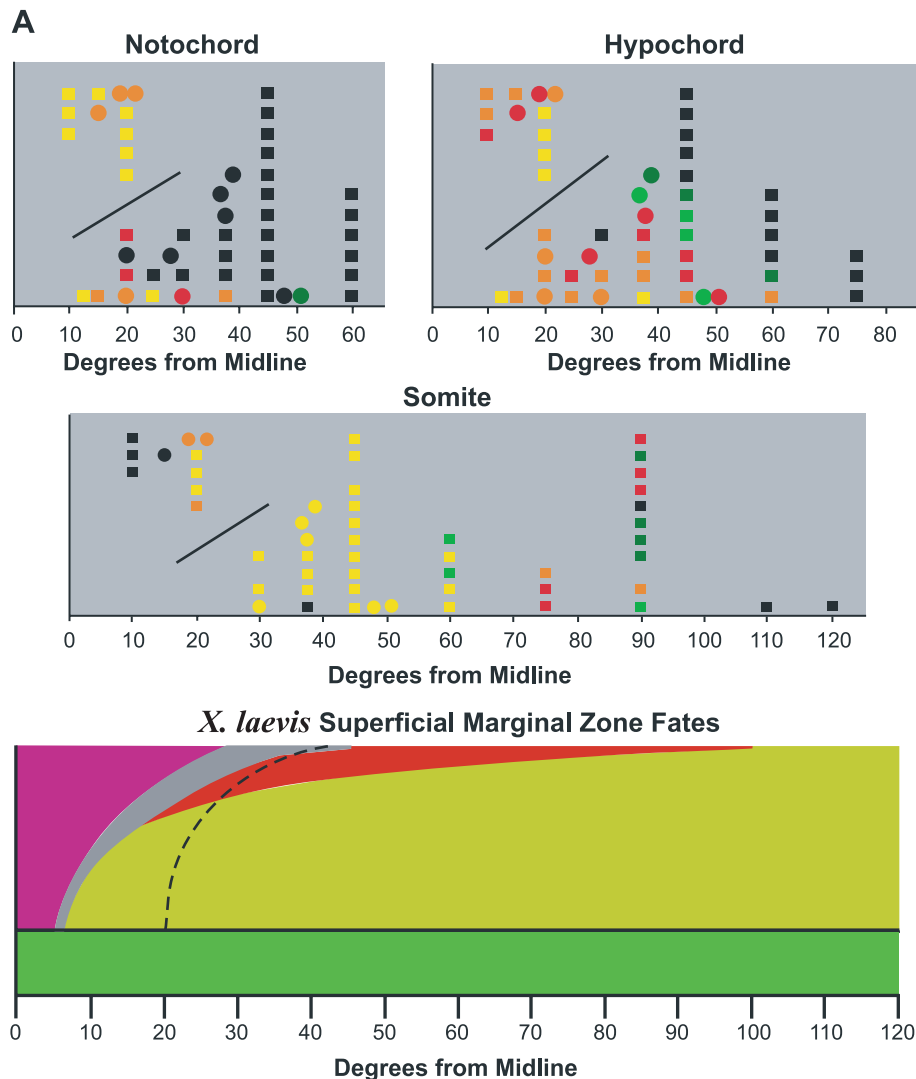


Fig. 9. Homotopic epithelial grafts into *X. laevis* (A) and *X. tropicalis* marginal zones define the approximate medial and lateral limits of superficial presumptive mesoderm tissues. Each point on the graphs (Notochord, Hypochord, Somite) represents the contribution of a single graft to those tissues, respectively. Large circles represent grafts measured from video images (estimated error at $\pm 3-5^\circ$), smaller squares represent grafts measured by eye (estimated error at $\pm 10-15^\circ$). Yellow = graft contributed to a span of many sections, with a few gaps of one to a few sections. Orange = graft contributed to a span of many sections but with several gaps of one to a few sections. Red = graft contributed to only a few or to sparsely scattered sections, with gaps of many sections. Green = graft contributed ambiguously to the tissue in question; Light Green = not clear, but could be the tissue in question; Dark Green = probably not the tissue in question, but rather label is in a nearby or related tissue. Black = no contribution. Points above and to the left of the diagonal bar represent the lateral endpoints of grafts that span the midline. Points below and to the right of the diagonal represent the medial endpoints of grafts that began away from the midline and extended laterally. The data for each graft are represented by a point in the same position on each of the three graphs; the vertical position of each point has no other meaning. Grafts that were not informative (e.g., due to poor histology) for a given tissue are not plotted on that graph. All grafts lateral of those shown on the graphs for Notochord and Hypochord had no contribution. The resulting maps of Superficial Marginal Zone Fates for *X. laevis* (A) or *X. tropicalis* (B) reflect our estimation of the medial–lateral beginning and ending points of each tissue type (color coded as in Fig. 2). We estimate that they are accurate to $\pm 10^\circ$. In addition, there may be between-embryo variation. The animal–vegetal extent of each tissue is estimated only from movies of giant explants; this lack of accuracy is reflected by the lack of a scale on the Y axis. The dashed line (A, Superficial Marginal Zone Fates) indicates the approximate position of the boundary between the deep presumptive notochordal and somitic tissues in *Xenopus laevis*.

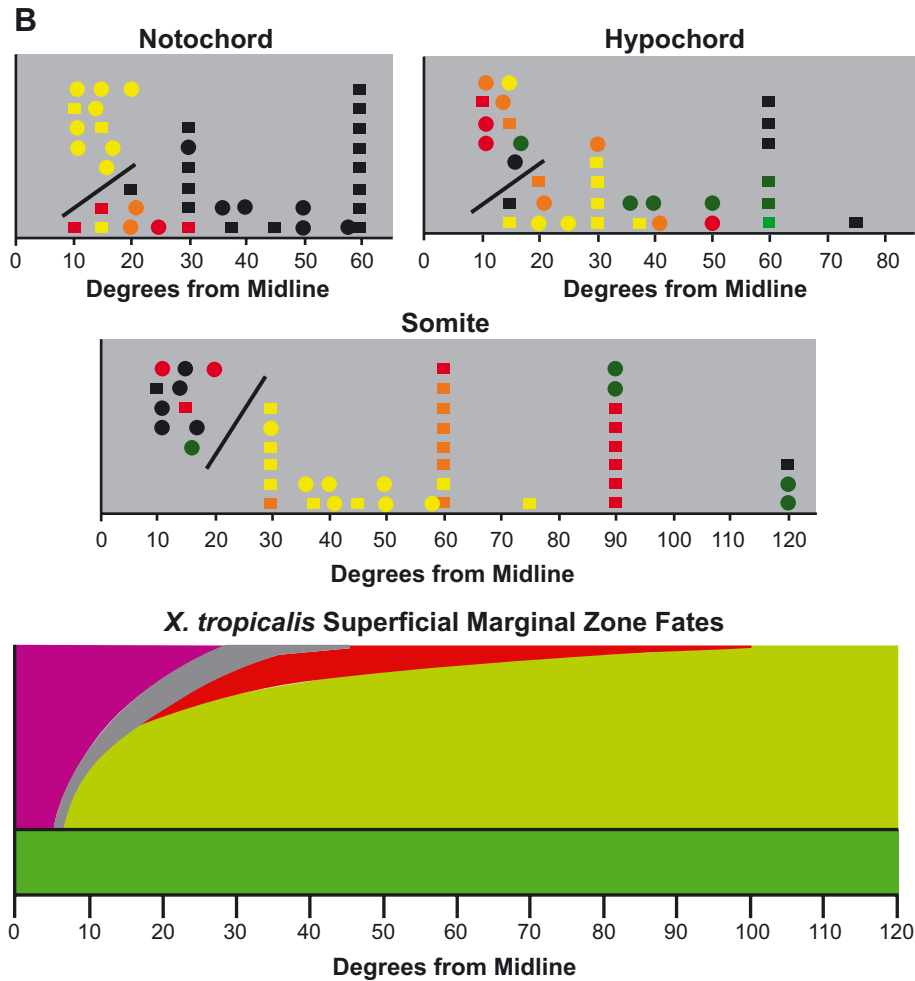


Fig. 9 (continued).

must be the hypochord. Supra-blastoporal endodermal cells continue converging on the dorsal midline, appearing to ingress, and several apparently deep cells are visible below the hypochord by stage 26 (data not shown) (see also plate 41, section A, in Hausen and Riebesell, 1991).

Discussion

Superficial mesoderm morphogenesis in Xenopus

X. laevis and *X. tropicalis* both have presumptive mesoderm in the superficial layer of the early gastrula, which contributes about 20% of the notochord, intercalated through most of its length by tailbud stage, and about 5% of the mid through posterior somites. One hundred percent of the hypochord originates superficially. The presumptive hypochord lays lateral and vegetal of the presumptive superficial notochord in the IMZ and the superficial component of the somitic mesoderm in turn originates laterally and vegetally to hypochord (Figs. 2A, 9). These tissues involute and converge and extend together to form

the midline of the mid and posterior gastrocoel roof (Fig. 2B). While the anterior deep presumptive notochordal tissues converge, extend and thicken, the anterior superficial tissues only converge and extend; thus by the end of gastrulation, the superficial presumptive notochord, which initially occupied a much narrower region of the marginal zone than the deep presumptive notochord, is only slightly narrower, with the presumptive hypochord overlapping the lateral edges of the deep notochord and the medial edges of the deep pre-somitic tissues. The superficial presumptive somitic cells initially ingress into the medial–ventral corner of the somites, adjacent to the notochord. The somitic cells of superficial origin integrate periodically along the length of the deep paraxial mesoderm and eventually stretch across the middle of the pre-somitic mesoderm; when the somites go through rotation during segmentation, the superficial cells come to rest at the horizontal myoseptum of the somite. Ingression of presumptive notochordal and somitic mesoderm into trunk tissues occurs primarily during neurulation, with the two rows of hypochord meeting along most of the midline and the LECs coming to abut the lateral edge of the hypochord

at about the same time the neural folds are meeting. Ingression into tail tissues probably continues for some time thereafter.

Hypochord ingression appears to follow directly at the conclusion of notochordal and somitic ingression, as documented for several anamniotes (Gibson, 1910, and references therein), and in *X. laevis* (Cleaver et al., 2000). Our mapping of the presumptive hypochord fits well with the observation that XHRT-1, a hairy and enhancer of split-related gene, is expressed in two rows of cells flanking those directly under the *X. laevis* notochord at stage 14 (Pichon et al., 2002, see their Fig. 2H) and later in the hypochord, as well as other tissues. It also fits well with the position of the presumptive hypochord in the zebrafish shield region between the presumptive notochord and presumptive somitic tissue (Latimer et al., 2002). After hypochord cells have ingressed, ingression, or at least strong dorsal midline convergence of supra-blastoporal endoderm cells apparently continues. The continuous dorsal convergence of the endoderm during neurulation and thereafter is congruent with the results of Chalmers and Slack (2000), who showed that the endoderm converges dorsally throughout its later morphogenesis.

The superficial presumptive somitic cells shear posteriorly with respect to the deep cells before ingressing

How the superficial presumptive somite is initially aligned with the deep presumptive somite has implications for its patterning and morphogenesis. The deep presumptive posterior notochord shears posteriorly with respect to the deep presumptive posterior somites. The superficial presumptive notochord, and presumably the hypochord, are strongly attached to the deep notochord by late gastrulation, and so shear posteriorly with it. By the time they ingress, the superficial presumptive somitic cells must be in register with the deep tissue into which they will ingress. Therefore, they must either begin in register with the deep presumptive somites (e.g., Fig. 8A, white dots), shearing with respect to the rest of the gastrocoel roof plate, or begin in register with the other gastrocoel roof plate tissues (e.g., Fig. 8A, *s) and move with these tissues, shearing only with respect to the deep presumptive somitic mesoderm.

The deep presumptive somitic mesoderm initially adjacent to the notochord will form about six somites when explanted; thus, we assume that in intact embryos, the future medial edges of only the first six presumptive myotomes initially lie adjacent to the presumptive notochord (Fig. 2A, dotted black lines; Fig. 8A, dashed black lines) (Shih and Keller, 1992c). The future medial edges of the remaining deep presumptive posterior somites are thus located progressively further away from the notochord, along the animal limit of the IMZ or “limit of involution” (Figs. 2A, 8A) (see Keller et al., 1992). During the end of gastrulation and through neurulation, as the posterior notochord

converges and extends, the future medial edge of the posterior deep presumptive somitic mesoderm will shear along the notochord–somite boundary, bringing the, now medial, edges of the presumptive posterior somites into alignment with the presumptive posterior notochord (compare Figs. 2A and 2B) (see Keller et al., 1991, 1992; Wilson et al., 1989).

The grafting experiments indicated that the superficial presumptive somite must shear posteriorly with respect to the deep presumptive somite before ingression. The superficial somitic cells originate both adjacent to the notochord and in more lateral regions of the IMZ (Fig. 9). However, they do not contribute to the first six myotomes, those initially lying adjacent to the deep presumptive notochord (Figs. 2A, 8A). The first four cranial myotomes (“head somites” in Nieuwkoop and Faber (1967)) as well as the first trunk somite and part of the second disappear before the metamorphosis (Chung et al., 1989; Nieuwkoop and Faber, 1967; Radice and Malacinski, 1989). Neither rhodamine label from transplanted grafts nor biotin label was ever seen in the head myotomes, or in the first two trunk somites, and only rarely in the next two. Thus, it appears, with respect to their pre-gastrulation organization, (Figs. 2A, 9) that the most medial superficial presumptive somitic cells will ingress into somites initially lying 25–35° laterally (prospective posterior). The lateral limit (prospective posterior end) of the superficial presumptive somites also lies medially of the most lateral (prospective posterior) deep presumptive somite (Fig. 2A), which was always labeled in biotinylated embryos. Thus, the entire gastrocoel roof plate shears posteriorly with respect to the deep presumptive somites, probably beginning anteriorly during gastrulation and continuing through neurulation, such that the superficial prospective somitic cells ingress into the deep layers as bottle cells, or by relamination, at progressively more posterior levels during mid to late neurulation. The middle and posterior supra-blastoporal endoderm have also been shown to shear posteriorly with respect to the underlying presumptive somitic mesoderm during neurulation (Keller, 1976). Thus, all the superficial tissues of the IMZ, and later the gastrocoel, are moving together, rather than shearing with respect to one another.

This behavior poses several interesting questions. First, why does any of the mesoderm, the somitic mesoderm in particular, originate superficially, such that just a few cells must be deposited in a specific region of each deep presumptive somite, by bottle cell ingression or relamination? Second, why does the superficial presumptive somitic mesoderm originate adjacent to the presumptive hypochord and notochord, rather than more posteriorly, over the corresponding deep component of the presumptive somite of which it will become a part? Why is it instead transported posteriorly with the extending notochord? Third, why doesn't the superficial presumptive somite contribute to anterior somites? We address these questions throughout the next four sections.

Are the superficial presumptive somitic cells presumptive slow muscle pioneer cells?

The surface-derived somitic cells in *Xenopus* may be homologous to a sub-population of the adaxial cells in zebrafish (Devoto et al., 1996), the slow muscle pioneer cells (Felsenfeld et al., 1991). Both originate near the presumptive notochord, separated by the presumptive hypochord (Latimer et al., 2002), both converge and extend with the presumptive notochord rather than the presumptive somitic mesoderm (Glickman et al., 2003), both eventually stretch across the medial–lateral span of the somites, and both wind up at the horizontal myoseptum of the segmented somite. A region homologous to the zebrafish adaxial cells is also found in the amniotes (reviewed in Sporle, 2001). Zebrafish slow muscle pioneer cells consist of two to six cells in the medial–ventral somite, adjacent to the notochord. They differentiate by forming actin fibrils much earlier than the rest of the muscle cells (Felsenfeld et al., 1991), and show strong, early expression of mRNAs for *myoD* (Devoto et al., 1996) and *engrailed* (Ekker et al., 1992; Hatta et al., 1991). The adaxial cells, but not the other somitic cells, are induced early by the notochord and depend on *sonic hedgehog* signaling from the notochord for their differentiation (Blagden et al., 1997).

Further characterization of these cells in amphibians will be required to establish morphological homology. Expression of homologous genes does not appear to be a useful criterion for homology in this case. For example, in zebrafish only the adaxial cells express *myoD* RNA until just before segmentation (Devoto et al., 1996; Weinberg et al., 1996), whereas *X. laevis* expresses *myoD* mRNA throughout the somites from the onset of gastrulation (Hopwood et al., 1989) and MyoD protein throughout the myotome from mid-gastrulation through somitogenesis (Hopwood et al., 1992). Zebrafish adaxial cells begin to express slow muscle myosin just before segmentation (Devoto et al., 1996), but in *X. laevis*, no slow muscle myosin is expressed until late tadpole stages (by stage 46, Elinson et al., 1999, by stage 40, D. Shook, unpublished data). Finally, we have not been able to detect *engrailed* expression in these cells in *X. laevis* at any stage (D. Shook, unpublished data), and 12/101, an antibody specific to fast muscle myosin in zebrafish (Devoto et al., 1996), stains the entire somite in *X. laevis* from stage 17 onward (Kintner and Brockes, 1984). Thus, whereas these cells appear to follow a similar morphogenic pathway in *X. laevis*, they do not appear to differentiate in the same way as in the zebrafish.

The adaxial cells in fish and amniotes may serve as “somitic sub-organizers” (Sporle, 2001). Consistent with this hypothesis, mutant fish embryos lacking slow muscle pioneer cells segment their somites, but lack horizontal myoseptae and have ventrally curved tails and U-shaped somites (e.g., Stickney et al., 2000) (reviewed in Barresi et al., 2000). If the cells described here are the amphibian homolog of the slow muscle pioneers, putative organizer

properties could be induced because of their superficial position in the IMZ. Their subsequent movements are regulated by the association of the gastrocoel roof plate with the notochord, as it shears posteriorly with respect to the deep presumptive somites. The morphogenesis of the adaxial cells in the zebrafish suggests that they too are linked to the notochord (Glickman et al., 2003). The notochord-mediated positioning of these cells would thus assure a spatially controlled role for them in patterning the somitic tissue after ingression. However, if the superficial presumptive somitic cells do have organizer properties, why is there no superficial contribution to the anterior six myotomes? Perhaps, the superficial cells gain their organizer properties via proximity to presumptive notochord (discussed in the next section), and since the presumptive anterior myotomes begin adjacent to the deep notochord, adaxial cells are induced in situ. Alternatively, the presumptive anterior myotomes may not need organizer cells, as they will either not form or not persist as somites. Finally, the adaxial cells in *Xenopus* may not be organizer cells at all.

Conservation of surface mesoderm; a role in patterning?

In most metazoans, mesoderm originates in the superficial layer of the embryo (Nielsen, 1995), requiring that it subsequently ingress or otherwise move into the deep layer, usually after gastrulation. In the two *Xenopus* species examined here, most of the presumptive mesoderm originates in the deep layer, thus avoiding the complication of having to internalize it (Fig. 1). Why originate any on the surface? The conservation of at least some surface mesoderm among amphibians suggests that selective pressure favors it, either because it plays a functional role by originating or remaining on the surface, or because it is an inevitable consequence of some other process (e.g., mesoderm specification or a mechanical requirement in morphogenesis, discussed in the following two sections). The superficial epithelial layer of the dorsal IMZ of the early *X. laevis* gastrula may be an essential component of the trunk organizer. Removing it in the early gastrula results in failure of convergent extension (Wilson, 1990), and grafting it to the ventral side of an early gastrula induces a second axis and convergent extension (Shih and Keller, 1992b).

Epithelial mesenchymal transition and ingression as a morphogenic design element in amphibian gastrulation

Ingression of a large number of cells from the surface epithelium raises several issues, discussed at length by Shook and Keller (2003). Cells must carefully regulate changes in gene expression, cell adhesion, and cell behavior as they go through an epithelial to mesenchymal transition (EMT) and ingression such that they do so in a highly patterned and progressive way, lest they form a significant wound in the embryo or disrupt its morphogenesis. The process of removing superficial cells from one layer and

adding them to another may also have biomechanical consequences and thus be a morphogenic design element in the concurrent morphogenic events of gastrulation and neurulation (Keller et al., 2003). As such, superficial mesoderm may persist because it allows more efficient morphogenesis.

Specification of mesoderm and endoderm in the marginal zone

The marginal zone is the only region of the early embryo where portions of the superficial epithelial layer will contribute to a different germ layer than the deep layer. In addition, the fraction of the superficial layer of the IMZ occupied by presumptive mesoderm varies greatly, from very low in *X. laevis* and *X. tropicalis* (this paper, Minsuk and Keller, 1997) to very high in the urodeles studied thus far (Delarue et al., 1992; Pasteels, 1942; Shook et al., 2002; Vogt, 1929). How do signaling pathways specify these different proportions of mesoderm and endoderm in the superficial IMZ of various amphibian species? And why do they only specify endoderm in the superficial layer? Higher TGF β signaling may specify endoderm whereas lower signaling specifies mesoderm (e.g., Clements et al., 1999). Perhaps, signaling occurs more efficiently in the epithelium causing TGF β signals from the vegetal endoderm to specify endoderm in part of the epithelial portion of the IMZ but exclusively mesoderm in the deep mesenchymal layer. Or if the marginal zone is initially specified as mesendoderm and only later resolved into mesoderm and endoderm (Rodaway and Patient, 2001), portions of the epithelial layer of the IMZ must preferentially receive a later signal directing endodermal specification, while the rest of the superficial layer and the deep layer receive signals for mesodermal differentiation. In *Pleurodeles*, a urodele, single cell marking experiments show that cells in the dorsal and dorsolateral IMZ are already restricted to a specific mesodermal fate by the early gastrula stage (Delarue et al., 1995); this may also hold true for *Xenopus*, although competence to make different types of mesoderm persists past this time (Domingo and Keller, 1995). The specification of the specific pattern of superficial mesoderm within the marginal zone of each species is even less well understood, although work in the zebrafish suggests that the Notch-Delta pathway is involved in specifying the hypochord (Latimer et al., 2002). The signals involved in specifying the organizer region as such may also specify part of the superficial layer as mesoderm.

Regulation of different early phenotypes in cells with a common presumptive fate

The dual origin and diverse morphogenic behaviors of cells with a common mesodermal fate presents a problem in regulation of cell behaviors. Superficial and deep presumptive mesoderm have very different morphogenic behaviors, yet are both differentiating toward a mesodermal

cell fate, suggesting that the cells have both common and distinct regulatory pathways, the first controlling cell specification and the second controlling cell behavior. The deep presumptive notochordal and somitic mesodermal cells show persistent stereotyped cell behaviors driving radial intercalation (Wilson and Keller, 1991; Wilson et al., 1989), and mediolateral intercalation (Shih and Keller, 1992a) beginning during gastrulation, whereas the corresponding superficial presumptive mesodermal cells retain their epithelial phenotype at least through their initial stages of differentiation as mesoderm. Once the superficial cells join the deep layers, they must participate in the continued differentiation of these tissues, including intercalation into the notochord. Therefore, these aspects of cell behavior, comprising epithelial and mesenchymal tissue organization, must be regulated independently of early mesodermal differentiation.

Inter-species variation in mechanisms of surface mesoderm morphogenesis appears substantial and may involve fundamental differences in cell behavior and biomechanics

We observed presumptive somitic cells ingressing as bottle cells in *X. laevis* but ingressing into the deep layer by relamination in *X. tropicalis*. The differences between bottle cell ingression and relamination may be substantial; we present a model of the cell behaviors that appear to be involved (Fig. 10). Relaminating cells do not actively constrict their apices (Figs. 10A–B), whereas bottle cells do (Figs. 10D–E), coupled with membrane internalization by endocytosis (Figs. 10D, E, blue membranes and vesicles). Thus, one difference between the two mechanisms probably lies in the organization of the apical actin cytoskeleton and regulation of its contraction. Relaminating cells integrate into and adopt the shapes and arrangement of the underlying tissue, indicating that they have adopted deep cell adhesion properties before ingression (Fig. 10B, red membranes), whereas ingressing bottle cells (Fig. 10E) only begin to intercalate into the somitic structure via basal protrusive activity during ingression, and become elongated apico-basally. We postulate that relamination and bottle cell ingression will require different regulation of cell adhesion molecules.

We postulate that relaminating cells do not actively ingress but rather first develop affinity for and integrate into the underlying somitic mesoderm (Fig. 10B, red membranes), while still part of the surface epithelium, and are subsequently actively covered over by the LECs (Fig. 10C, arrows). Ingressing bottle cells, on the other hand, actively constrict their apices (Fig. 10D, small arrows) and draw the lateral endodermal crests passively toward the midline (Fig. 10E, large arrow). Finally, the ingressing bottle cells withdraw from the surface layer (Fig. 10F, small arrows).

Relamination implies a major change in cell polarity and re-targeting of adhesion molecules to the apical surface

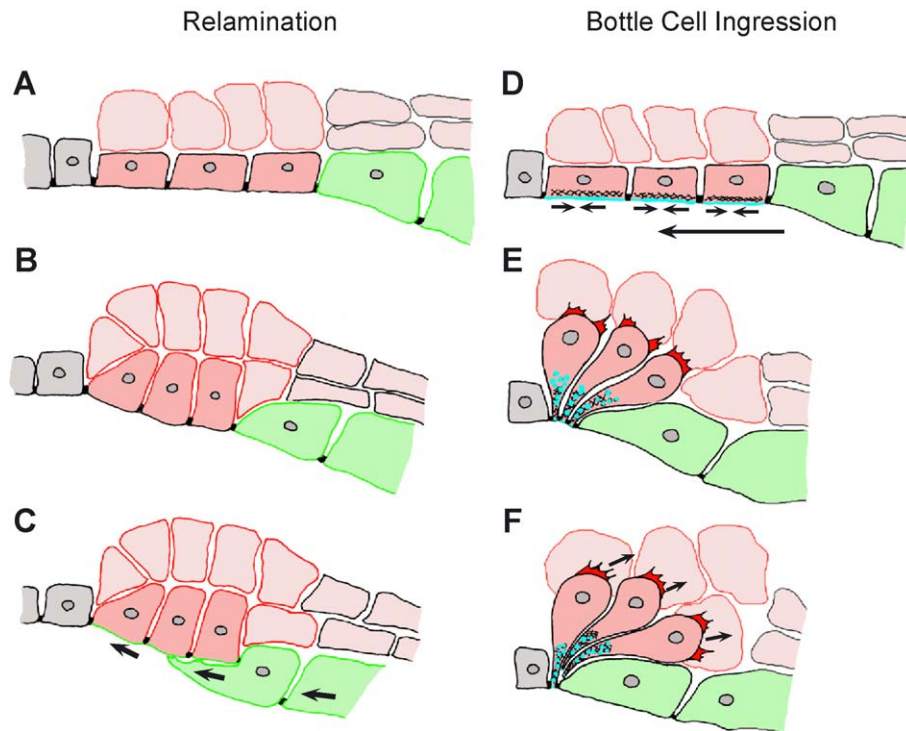


Fig. 10. Shows the hypothesized progression of cell behaviors during relamination (A–C) or bottle cell ingressions (D–F). In relamination, superficial presumptive mesodermal cells (dark pink) first integrate into the underlying mesodermal tissues (light pink) (B), expressing compatible adhesion molecules (red) basally. The superficial presumptive mesodermal cells then express an adhesion molecule apically (green) that is compatible with subsequent endodermal migration over their apical face (C). In bottle cell ingressions, cells first constrict their apical domains (D, E) and internalize their apical membrane (blue). This draws the endoderm medially (E). Cells subsequently ingress out of the epithelial layer, releasing their apical junctions (F).

during protein trafficking within these cells. These cells may undergo two changes in adhesion. The first, involving their basolateral surfaces, would mediate their participation in somitic mesoderm formation (Fig. 10B, red membranes) and the second, involving their apical surfaces, would mediate traction by the lateral endodermal cells (Fig. 10C, green membranes). Whether the relaminating cells maintain their tight junctions while allowing migration over their surfaces is not known.

Further differences between the two species in the biomechanical and cell-level organization of these tissues, e.g., in the strength of the cell–cell adhesiveness, or in the cytoskeletal architecture integrating the cell sheet, are suggested by the morphology of their gastrocoel roof plates. *X. laevis* lacks the distinction between zones I and II of the gastrocoel roof plate observed in *X. tropicalis*, which may be related to the more tightly packed and flatter appearance of these cells in *X. laevis* (compare Figs. 5A and 5C). There are also timing differences: *X. tropicalis* begins ingressions earlier, specifically at stage 13 instead of 15 for *X. laevis*.

These differences could be necessitated by the nature of the relamination mechanism of mesoderm formation, or it could be an independent variable, or perhaps one linked to some other parameter of mesoderm development, such as somite formation, which is also highly variable among amphibians (see Keller, 2000).

Evolution of bottle cell ingressions and relamination

Relamination in *X. tropicalis* resembles that in *Hymenochirus boettgeri* (Minsuk and Keller, 1996), in the sister genus of the *Xenopus* group, suggesting that the different mechanisms found in *X. laevis* arose in conjunction with its switch to tetraploidy. This divergence of developmental mechanism between sister species suggests that it is either under little stabilizing selective pressure or under selective pressure from an environmental or intrinsic embryonic source stronger than any stabilizing selection. An environmental source could be the apparent adaptation of *X. laevis* to tolerate higher salinity than does *X. tropicalis* (Tinsley et al., 1996), which might require different epithelial character for proper ionic regulation. An embryonic source might be the difference in cell number or size; *X. laevis* is about six times larger than *X. tropicalis* with cells roughly twice the volume (Minsuk, 1995), giving it about three times as many cells at the onset of gastrulation. Any or all of these related differences could affect the mechanics and architecture of surface mesoderm morphogenesis. In any event, the superficial presumptive somitic cells of both species, regardless of ingressions mechanism, wind up in the horizontal myoseptum, suggesting that, whereas the general patterns of morphogenesis toward the basic body plan at the “phylo-typic stage” are conserved, the specific cellular mechanisms of morphogenesis are more flexible. It is only the cellular

mechanism by which cells ingress that is divergent; ingression of epithelial cells into the mesodermal layer during neurulation appears to be primitive for anurans (Bolker, 1993; Delarue et al., 1994; Minsuk and Keller, 1996, 1997; Pasteels, 1942; Purcell and Keller, 1993; Shook et al., 2002; Vogt, 1929).

The lack of conservation in the cellular mechanism of surface mesoderm ingression between these closely related species is somewhat surprising, given the generally assumed conservation of early development, but fits with the developmental hourglass concept, which posits that development is more conserved closer to the phylotypic stage (for *Xenopus*, a few hours after neurulation is complete), when the greatest number of patterning interactions occur (and toward which the general patterning events of early development are directed), with progressively greater divergence allowed during progressively earlier or later development (for a discussion of this assumption and the developmental hourglass, see Raff, 1996).

That the level where the variation is occurring is in cell mechanism is not surprising. In a hierarchy of developmental effect, patterning decisions are at the top, while effectors of that patterning, as by specific cell behaviors, are at the bottom. Changes at the top of the developmental hierarchy may have effects on many elements of development, and so

should be successful less often, while those at the bottom of the hierarchy may only effect the tissue in which they occur, and so may succeed more often. This idea is supported by the finding that upstream genes in an epistatic pathway are less variable than downstream genes (Lu and Rausher, 2003; Rausher et al., 1999). Rudel and Sommer (2003) have also observed that cellular mechanisms are “more complaisant for changes and co-option than complex signaling systems”, and argue that cellular mechanisms are in some sense autonomous, and can thus act as “cassettes” that can be used interchangeably to allow developmental evolution. Thus, adaptive responses to environmental selective pressures might most frequently be by variation in cell biology or behavior, with variation higher in the hierarchy, at the level of patterning, occurring less frequently and thus being seen at deeper levels of phylogenetic divergence.

Surface presumptive mesoderm on the gastrocoel roof: an ancestral character in chordates?

With our results, all chordates examined have presumptive superficial mesoderm in their pregastrular fate maps, either in the epiblast of the amniotes or in the superficial layer of the anamniotes. The retention of presumptive mesoderm in the epithelial surface of the gastrocoel roof

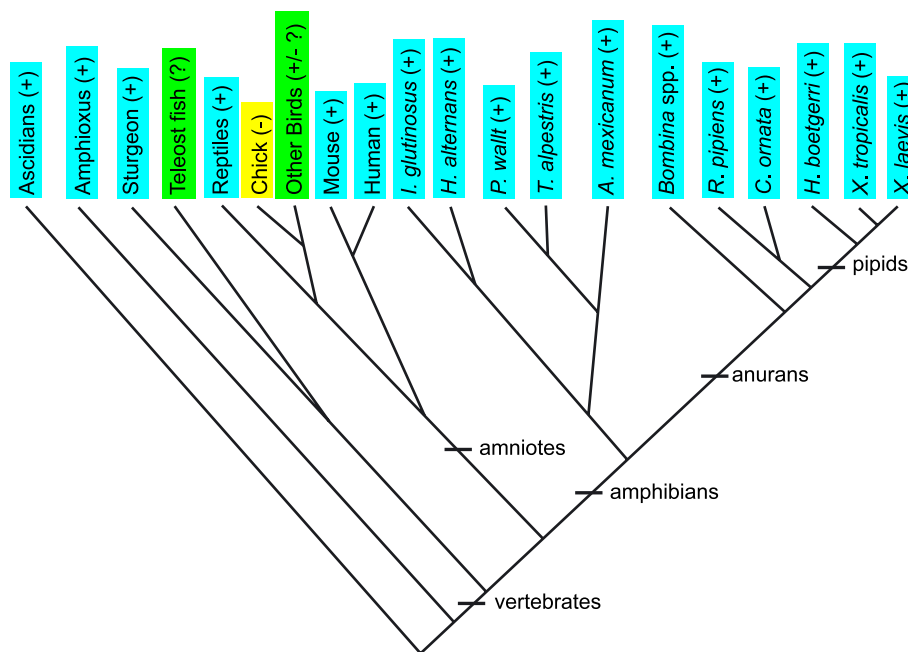


Fig. 11. Distribution of the character of having superficial mesoderm in the gastrocoel roof (e.g., a gastrocoel roof plate) among the chordates. Phylogenetic ordering of the amphibians is based on published work (Cannatella and De Sa, 1993; De Sa and Hillis, 1990; Duellman and Trueb, 1994). Blue highlighting indicates the presence of superficial mesoderm, yellow indicates negative cases, and green indicates ambiguous cases. Ascidiens (Berrill, 1950; Conklin, 1905; Satoh, 1978); amphioxus (Conklin, 1932); sturgeon (Bolker, 1993); zebrafish (Kimmel et al., 1995; Warga and Nusslein-Volhard, 1999); chick (Jurand, 1962; Sausedo and Schoenwolf, 1993); other birds (Balfour, 1885; Nelsen, 1953); reptiles (Nelsen, 1953, and references therein); mouse (Sulik et al., 1994); human (O’Rahilly and Müller, 1987); the gymnophionans *Ichthyophis glutinosus* (Sarasin and Sarasin, 1887–1890) and *Hypogeophis alternans* (Brauer, 1897); the urodeles *Pleurodeles waltl* (Delarue et al., 1992, 1995; Vogt, 1929); *Triturus alpestris* (Vogt, 1929); *Ambystoma mexicanum* (Pasteels, 1942; Shook et al., 2002; Smith and Malacinski, 1983); and the anurans *Bombina* spp. (Vogt, 1929); *Rana pipiens* (Delarue et al., 1994); *Ceratophrys ornata* (Purcell and Keller, 1993); *Hymenochirus boetgeri* (Minsuk and Keller, 1996); *Xenopus tropicalis*, this paper; *Xenopus laevis* (Minsuk and Keller, 1997; this paper).

after gastrulation has also been documented for several chordates (Fig. 11), suggesting that this too is an ancestral character, and thus of general interest in understanding chordate development.

We propose that the gastrocoel roof plate described here is, in part, homologous to the notochordal plate of the mouse (Sulik et al., 1994), differing from notochordal plate in that it contains both presumptive notochordal, hypochordal, and somitic cells. Both the gastrocoel roof plate and the notochordal plate consist of presumptive mesodermal cells that remain transiently in the roof of the gastrocoel after involution around the dorsal blastoporal lip or ingression through the node. Both the notochordal plate (Sulik et al., 1994) and the gastrocoel roof plate have a single cilium at the posterior edge of each cell, supporting the homology of the two structures. These cilia may function in determining the left–right axis of mice (e.g., Nonaka et al., 1998) (but see also Mercola and Levin, 2001; Wagner and Yost, 2000). Whether the cilia themselves or the internal cellular polarity they represent play a similar role in amphibians is not known. The gastrocoel roof plate maintains its epithelial state and involutes as such, whereas the notochordal plate presumably de-epithelializes as it moves from the epithelial epiblast of the node, through the node as a mesenchyme, and out into the subgerminal cavity where it appears to re-epithelialize to form the notochordal plate.

The teleost fish appears to have fairly divergent early development, lacking any proper embryonic epithelium during gastrulation, and having no gut cavity until much later in development, well after notochordal differentiation (Wallace and Pack, 2003); thus, there is no gastrocoel roof epithelium for presumptive mesodermal cells to be retained in. The chick is a clear exception to the conservation of the gastrocoel roof plate (Fig. 11), having no mesodermal component in the epithelial roof of its archenteron (Jurand, 1962; Sausedo and Schoenwolf, 1993), and having no population of monociliated cells analogous to the mouse notochordal plate (Manner, 2001). In other amniotes, such as at least some reptiles, there appears to be a well-defined blastopore in the node region over which the notochordal plate involutes (Balfour, 1885; Nelsen, 1953); in humans, there is an open notochordal canal that runs in from the node to connect it to the hollow notochordal process, which eventually gives rise to a notochordal plate after fusing with the underlying endoderm (O’Rahilly and Müller, 1987), which turns the notochordal canal into a neurenteric canal, analogous to an amphibian blastopore. The presence of a reptilian blastopore and observations of a transient or cryptic neurenteric canal in some birds and a persistent neurenteric canal in humans suggests that the avian and mammalian node, if not the entire primitive streak, evolved from a blastoporal structure (Arendt and Nubler-Jung, 1999; Balfour, 1885). That this morphology is so broadly conserved suggests again that the tissues making up the notochordal or gastrocoel roof plate, if not the blastopore itself, play some important role in development (discussed above for amphib-

ians). As these tissues initially belong to the organizer, it is tempting to speculate that they continue in this capacity through later development. It would be very interesting to understand why some amniotes, such as the chick, have lost their gastrocoel roof plate, and how they might have compensated for this loss.

Acknowledgments

We would like to thank Max Ezin and Lance Davidson for helpful comments and discussion of the manuscript. This work was funded by NIH NRSA 5-F32-HD 08183 to D. Shook and NIH RO1 HD 25594 and RO1 HD 36426 to R. Keller.

References

- Arendt, D., Nubler-Jung, K., 1999. Rearranging gastrulation in the name of yolk: evolution of gastrulation in yolk-rich amniote eggs. *Mech. Dev.* 81, 3–22.
- Baker, P.C., 1965. Fine structure and morphogenic movements in the gastrula of the treefrog, *Hyla regilla*. *J. Cell Biol.* 24, 95–116.
- Balfour, F.M., 1885. *A Treatise on Comparative Embryology*. Vertebrata, vol. II. Macmillan, London.
- Balinsky, B.I., 1961. Ultrastructural mechanisms of gastrulation and neurulation. Symposium on Germ Cells and Development. Institut Internazionale d’Embryologie and Fondazione A. Baselli, Pallanza, pp. 560–563.
- Ballard, W.W., 1973. A new fate map for *Salmo gairdneri*. *J. Exp. Zool.* 184, 49–74.
- Ballard, W.W., 1980. Morphogenetic movements in *Acipenserid* embryos. *J. Exp. Zool.* 213, 69–103.
- Barresi, M.J., Stickney, H.L., Devoto, S.H., 2000. The zebrafish slow-muscle-omitted gene product is required for Hedgehog signal transduction and the development of slow muscle identity. *Development* 127, 2189–2199.
- Bauer, D.V., Huang, S., Moody, S.A., 1994. The cleavage stage origin of Spemann’s organizer: analysis of the movements of blastomere clones before and during gastrulation in *Xenopus*. *Development* 120, 1179–1189.
- Berrill, N.J., 1950. *The Tunicata with an Account of the British Species*. Ray Society, London.
- Blagden, C.S., Currie, P.D., Ingham, P.W., Hughes, S.M., 1997. Notochord induction of zebrafish slow muscle mediated by Sonic hedgehog. *Genes Dev.* 11, 2163–2175.
- Bolker, J.A., 1993. Gastrulation and mesoderm morphogenesis in the white sturgeon. *J. Exp. Zool.* 266, 116–131.
- Brauer, A., 1897. Beitrage zur kenntnis der entwicklungsgeschichte und der anatomie der gymnophionen. *Zool. Jahrb. Anat.* 10, 277–279, 389–472.
- Cannatella, D.C., De Sa, R.O., 1993. *Xenopus laevis* as a model organism. *Syst. Biol.* 42, 476–507.
- Chalmers, A.D., Slack, J.M., 2000. The *Xenopus* tadpole gut: fate maps and morphogenetic movements. *Development* 127, 381–392.
- Chalmers, A.D., Strauss, B., Papalopulu, N., 2003. Oriented cell divisions asymmetrically segregate aPKC and generate cell fate diversity in the early *Xenopus* embryo. *Development* 130, 2657–2668.
- Chung, H.M., Neff, A.W., Malacinski, G.M., 1989. Autonomous death of amphibian *Xenopus laevis* cranial myotomes. *J. Exp. Zool.* 251, 290–299.
- Cleaver, O., Seufert, D.W., Krieg, P.A., 2000. Endoderm patterning by the

- notochord: development of the hypochord in *Xenopus*. *Development* 127, 869–879.
- Clements, D., Friday, R.V., Woodland, H.R., 1999. Mode of action of VegT in mesoderm and endoderm formation. *Development* 126, 4903–4911.
- Conklin, E.G., 1905. The organization and cell lineage of the ascidian egg. *J. Acad. Nat. Sci. (Phila.)* 13, 1–119.
- Conklin, E.G., 1932. The embryology of *Amphioxus*. *J. Morphol.* 54, 69–151.
- Dale, L., Slack, J.M., 1987. Fate map for the 32-cell stage of *Xenopus laevis*. *Development* 99, 527–551.
- De Sa, R.O., Hillis, D.M., 1990. Phylogenetic relationships of the pipid frogs *Xenopus* and *Silurana*: an integration of ribosomal DNA and morphology. *Mol. Biol. Evol.* 7, 365–376.
- Delarue, M., Sanchez, S., Johnson, K.E., Darribère, T., Boucaut, J.C., 1992. A fate map of superficial and deep circumblastoporal cells in the early gastrula of *Pleurodeles waltlii*. *Development* 114, 135–146.
- Delarue, M., Johnson, K.E., Boucaut, J.C., 1994. Superficial cells in the early gastrula of *Rana pipiens* contribute to mesodermal derivatives. *Dev. Biol.* 165, 702–715.
- Delarue, M., Saez, F.J., Johnson, K.E., Boucaut, J.C., 1995. Restriction of cell fate of superficial cells in the marginal zone of the amphibian embryo *Pleurodeles waltlii*. *J. Exp. Zool.* 273, 303–316.
- Devoto, S.H., Melancon, E., Eisen, J.S., Westerfield, M., 1996. Identification of separate slow and fast muscle precursor cells in vivo, prior to somite formation. *Development* 122, 3371–3380.
- Domingo, C., Keller, R., 1995. Induction of notochord cell intercalation behavior and differentiation by progressive signals in the gastrula of *Xenopus laevis*. *Development* 121, 3311–3321.
- Duellman, W.E., Trueb, L., 1994. *The Biology of Amphibians*. The Johns Hopkins Univ. Press, Baltimore.
- Ekker, M., Wegner, J., Akimenko, M.A., Westerfield, M., 1992. Coordinate embryonic expression of three zebrafish engrailed genes. *Development* 116, 1001–1010.
- Elinson, R.P., Remo, B., Brown, D.D., 1999. Novel structural elements identified during tail resorption in *Xenopus laevis* metamorphosis: lessons from tailed frogs. *Dev. Biol.* 215, 243–252.
- Elul, T., Koehl, M.A.R., Keller, R., 1997. Cellular mechanism underlying neural convergent extension in *Xenopus laevis* embryos. *Dev. Biol.* 191, 243–258.
- Felsenfeld, A.L., Curry, M., Kimmel, C.B. (1991). The fub-1 mutation blocks initial myofibril formation in zebrafish muscle pioneer cells.
- Gibson, W.T., 1910. The development of the hypochord in *Raia batis*; with a note upon the occurrence of the epibranchial groove in amniote embryos. *Anat. Anz.* 35, 407–428.
- Glickman, N.S., Kimmel, C.B., Jones, M.A., Adams, R.J., 2003. Shaping the zebrafish notochord. *Development* 130, 873–887.
- Hamilton, L., 1969. The formation of somites in *Xenopus laevis*. *J. Embryol. Exp. Morphol.* 22, 253–264.
- Hatta, K., Bremiller, R., Westerfield, M., Kimmel, C.B. (1991). Diversity of expression of engrailed-like antigens in zebrafish.
- Hausen, P., Riebesell, M., 1991. *The Early Development of Xenopus laevis: An Atlas of Histology*. Springer-Verlag, Berlin.
- Hopwood, N.D., Pluck, A., Gurdon, J.B., 1989. MyoD expression in the forming somites is an early response to mesoderm induction in *Xenopus* embryos. *EMBO J.* 8, 3409–3418.
- Hopwood, N.D., Pluck, A., Gurdon, J.B., Dilworth, S.M., 1992. Expression of XMyoD protein in early *Xenopus laevis* embryos. *Development* 114, 31–38.
- Jurand, A., 1962. The development of the notochord in chick embryos. *J. Embryol. Exp. Morphol.* 10, 602–621.
- Kay, B.K., Peng, H.B., 1991. *Methods in Cell Biology*. Academic Press, New York.
- Keller, R.E., 1975. Vital dye mapping of the gastrula and neurula of *Xenopus laevis*: I. Prospective areas and morphogenetic movements of the superficial layer. *Dev. Biol.* 42, 222–241.
- Keller, R.E., 1976. Vital dye mapping of the gastrula and neurula of *Xenopus laevis*: II. Prospective areas and morphogenetic movements of the deep layer. *Dev. Biol.* 51, 118–137.
- Keller, R.E., 1978. Timelapse cinematography of superficial cell behaviour during and prior to gastrulation in *Xenopus laevis*. *J. Morphol.* 157, 223–247.
- Keller, R., 2000. The origin and morphogenesis of amphibian somites. *Curr. Top. Dev. Biol.* 47, 183–246.
- Keller, R., Tibbetts, P., 1989. Mediolateral cell intercalation in the dorsal, axial mesoderm of *Xenopus laevis*. *Dev. Biol.* 131, 539–549.
- Keller, R., Shih, J., Wilson, P.A., Sater, A.K., 1991. Patterns of cell motility, cell interactions, and mechanisms during convergent extension in *Xenopus*. In: Gerhart, G.C. (Ed.), *Cell–Cell Interactions in Early Development*. Society for Developmental Biology, 49th Symposium, Academic Press, New York, pp. 31–62.
- Keller, R., Shih, J., Domingo, C., 1992. The patterning and functioning of protrusive activity during convergence and extension of the *Xenopus* organiser. *Dev., Suppl.*, 81–91.
- Keller, R., Poznanski, A., Elul, T., 1999. Experimental embryological methods for analysis of neural induction in the amphibian. *Methods Mol. Biol.* 97, 351–392.
- Keller, R., Davidson, L., Edlund, A., Elul, T., Ezin, M., Shook, D., Skoglund, P., 2000. Mechanisms of convergence and extension by cell intercalation. *Philos. Trans. R. Soc. Lond., Ser. B Biol. Sci.* 355, 897–922.
- Keller, R., Davidson, L.A., Shook, D.R., 2003. How we are shaped: the biomechanics of gastrulation. *Differentiation* 71, 171–205.
- Kimmel, C.B., Warga, R.M., Schilling, T.F., 1990. Origin and organization of the zebrafish fate map. *Development* 108, 581–594.
- Kimmel, C.B., Ballard, W.W., Kimmel, S.R., Ullmann, B., Schilling, T.F., 1995. Stages of embryonic development of the Zebrafish. *Dev. Dyn.* 203, 253–310.
- Kintner, C.R., Brockes, J.P., 1984. Monoclonal antibodies identify blastemal cells derived from dedifferentiating muscle in newt limb. *Nature* 308, 67–69.
- Latimer, A.J., Dong, X., Markov, Y., Appel, B., 2002. Delta-Notch signaling induces hypochord development in zebrafish. *Development* 129, 2555–2563.
- Lawson, K.A., Meneses, J.J., Pedersen, R.A., 1991. Clonal analysis of epiblast fate during germ layer formation in the mouse embryo. *Development* 113, 891–911.
- Linker, C., Bronner-Fraser, M., Mayor, R., 2000. Relationship between gene expression domains of Xsnail, Xslug, and Xtwist and cell movement in the prospective neural crest of *Xenopus*. *Dev. Biol.* 224, 215–225.
- Lofberg, J., 1974. Apical surface topography of invaginating and noninvaginating cells. A scanning-transmission study of amphibian neurulae. *Dev. Biol.* 36, 311–329.
- Lu, Y., Rausher, M.D., 2003. Evolutionary rate variation in anthocyanin pathway genes. *Mol. Biol. Evol.* 20, 1844–1853.
- Manner, J., 2001. Does an equivalent of the “ventral node” exist in chick embryos? A scanning electron microscopic study. *Anat. Embryol. (Berl)* 203, 481–490.
- Mayor, R., Morgan, R., Sargent, M.G., 1995. Induction of the prospective neural crest of *Xenopus*. *Development* 121, 767–777.
- Mercola, M., Levin, M., 2001. Left–right asymmetry determination in vertebrates. *Annu. Rev. Cell Dev. Biol.* 17, 779–805.
- Minsuk, S.B., 1995. *A Comparative Study of Gastrulation and Mesoderm Formation in Pipid Frogs*. PhD Thesis, University of California, Berkeley.
- Minsuk, S.B., Keller, R.E., 1996. Dorsal mesoderm has a dual origin and forms by a novel mechanism in *Hymenochirus*, a relative of *Xenopus*. *Dev. Biol.* 174, 92–103.
- Minsuk, S.B., Keller, R.E., 1997. Surface mesoderm in *Xenopus*: a revision of the stage 10 fate map. *Dev. Genes Evol.* 207, 389–401.
- Muller, H.A., Hausen, P., 1995. Epithelial cell polarity in early *Xenopus* development. *Dev. Dyn.* 202, 405–420.
- Nelsen, O.E., 1953. *Comparative Embryology of the Vertebrates*. The Blakiston, New York.

- Nielsen, C., 1995. *Animal Evolution. Interrelationships of the Living Phyla*. Oxford Univ. Press, Oxford.
- Nieuwkoop, P.D., Faber, J., 1967. *Normal Table of Xenopus laevis* (Daudin). North Holland Publishing, Amsterdam.
- Nieuwkoop, P.D., Sutasurya, L.A., 1979. *Primordial Germ Cells in the Chordates; Embryogenesis and Phylogenesis*. Cambridge Univ. Press, Cambridge.
- Nonaka, S., Tanaka, Y., Okada, Y., Takeda, S., Harada, A., Kanai, Y., Kido, M., Hirokawa, N., 1998. Randomization of left–right asymmetry due to loss of nodal cilia generating leftward flow of extraembryonic fluid in mice lacking KIF3B motor protein. *Cell* 95, 829–837.
- O’Rahilly, R., Müller, F., 1987. *Developmental Stages in Human Embryos*. Carnegie Institution of Washington, Washington, DC.
- Pasteels, J., 1942. New observations concerning the maps of presumptive areas of the young amphibian gastrula (*Amblystoma* and *Discoglossus*). *J. Exp. Zool.* 89, 255–281.
- Perry, M.M., Waddington, C.H., 1966. Ultrastructure of the blastopore cells in the newt. *J. Embryol. Exp. Morphol.* 15, 317–330.
- Pichon, B., Taelman, V., Kricha, S., Christophe, D., Bellefroid, E.J., 2002. XHRT-1, a hairy and Enhancer of split related gene with expression in floor plate and hypochord during early *Xenopus* embryogenesis. *Dev. Genes Evol.* 212, 491–495.
- Poznanski, A., Keller, R., 1997. The role of planar and early vertical signaling in patterning the expression of Hoxb-1 in *Xenopus*. *Dev. Biol.* 184, 351–356.
- Poznanski, A., Minsuk, S., Stathopoulos, D., Keller, R., 1997. Epithelial cell wedging and neural trough formation are induced planarly in *Xenopus*, without persistent vertical interactions with mesoderm. *Dev. Biol.* 189, 256–269.
- Psychoyos, D., Stern, C.D., 1996. Fates and migratory routes of primitive streak cells in the chick embryo. *Development* 122, 1523–1534.
- Purcell, S.M., Keller, R., 1993. A different type of amphibian mesoderm morphogenesis in *Ceratophrys ornata*. *Development* 117, 307–317.
- Radice, G.P., Malacinski, G.M., 1989. Expression of myosin heavy chain transcripts during *Xenopus laevis* development. *Dev. Biol.* 133, 562–568.
- Raff, R.A., 1996. *The Shape of Life: Genes, Development, and the Evolution of Animal Form*. The University of Chicago Press, Chicago.
- Rausher, M., Miller, R., Tiffin, P., 1999. Patterns of evolutionary rate variation among genes of the anthocyanin biosynthetic pathway. *Mol. Biol. Evol.* 16, 266–274.
- Rodaway, A., Patient, R., 2001. Mesendoderm: an ancient germ layer? *Cell* 105, 169–172.
- Rudel, D., Sommer, R.J., 2003. The evolution of developmental mechanisms. *Dev. Biol.* 264, 15–37.
- Sarasin, P., Sarasin, F., 1887–1890. Zur entwicklungsgeschichte und anatomie der Ceylonesischen blindwuhle, *Ichthophis glustinosa*. *Ergebn. Natur. Forsh. Ceylon* 1884–1886. C.W. Kreidel’s, Wiesbaden.
- Satoh, N., 1978. Cellular morphology and architecture during early morphogenesis of the ascidian egg: an SEM study. *Biol. Bull.* 155, 608–614.
- Sausedo, R.A., Schoenwolf, G.C., 1993. Cell behaviors underlying notochord formation and extension in avian embryos: quantitative and immunocytochemical studies. *Anat. Rec.* 237, 58–70.
- Schoenwolf, G.C., Garcia, M.-V., Dias, M.S., 1992. Mesoderm movement and fate during avian gastrulation and neurulation. *Dev. Dyn.* 193, 235–248.
- Schroeder, T.E., 1970. Neurulation in *Xenopus laevis*. An analysis and model based upon light and electron microscopy. *J. Embryol. Exp. Morphol.* 23, 427–462.
- Shih, J., Fraser, S.E., 1995. Distribution of tissue progenitors within the shield region of the zebrafish gastrula. *Development* 121, 2755–2765.
- Shih, J., Keller, R., 1992a. Cell motility driving mediolateral intercalation in explants of *Xenopus laevis*. *Development* 116, 901–914.
- Shih, J., Keller, R., 1992b. The epithelium of the dorsal marginal zone of *Xenopus* has organizer properties. *Development* 116, 887–899.
- Shih, J., Keller, R., 1992c. Patterns of cell motility in the organizer and dorsal mesoderm of *Xenopus laevis*. *Development* 116, 915–930.
- Shook, D.R., Keller, R., 2003. Mechanisms, mechanics and function of epithelial mesenchymal transitions in early development. *Mech. Dev.* 120, 1351–1383.
- Shook, D.R., Majer, C., Keller, R., 2002. Urodeles remove mesoderm from the superficial layer by subduction through a bilateral primitive streak. *Dev. Biol.* 248, 220–239.
- Smith, J.C., Malacinski, G.M., 1983. The origin of the mesoderm in an Anuran, *Xenopus laevis* and a Urodele, *Ambystoma mexicanum*. *Dev. Biol.* 98, 250–254.
- Sporle, R., 2001. Epaxial–adaxial–hypaxial regionalisation of the vertebrate somite: evidence for a somitic organiser and a mirror-image duplication. *Dev. Genes Evol.* 211, 198–217.
- Stickney, H.L., Barresi, M.J., Devoto, S.H., 2000. Somite development in zebrafish. *Dev. Dyn.* 219, 287–303.
- Sulik, K., Dehart, D.B., Inagaki, T., Carson, J.L., Vrablic, T., Gesteland, K., Schoenwolf, G.C., 1994. Morphogenesis of the murine node and notochordal plate. *Dev. Dyn.* 201, 260–278.
- Tinsley, R.C., Loumont, C., Kobel, H.R., 1996. Geographical distribution and ecology. In: Tinsley, R.C., Kobel, H.R. (Eds.), *The Biology of Xenopus*. Calrendon Press, Oxford, pp. 35–59.
- Vodicka, M.A., Gerhart, J.C., 1995. Blastomere derivation and domains of gene expression in the Spemann organizer of *Xenopus laevis*. *Development* 121, 3505–3518.
- Vogt, W., 1929. Gestaltungsanalyse am Amphibienkiem Mit Ortlicher Vitalfarbung: II. Teil. Gastrulation und Mesoderbildung Bei Urodelen und Anuren. *Wilhelm Roux’ Arch. Entwicklungsmech. Org.* 120, 384–601.
- Wagner, M.K., Yost, H.J., 2000. Left–right development: the roles of nodal cilia. *Curr. Biol.* 10, R149–R151.
- Wallace, K.N., Pack, M., 2003. Unique and conserved aspects of gut development in zebrafish. *Dev. Biol.* 255, 12–29.
- Warga, R.M., Nusslein-Volhard, C., 1999. Origin and development of the zebrafish endoderm. *Development* 126, 827–838.
- Weinberg, E.S., Allende, M.L., Kelly, C.S., Abdelhamid, A., Murakami, T., Andermann, P., Doerre, O.G., Grunwald, D.J., Riggleman, B., 1996. Developmental regulation of zebrafish MyoD in wild-type, no tail and spadetail embryos. *Development-Cambridge* 122, 271–280.
- Wilson, P., 1990. *The Development of the Axial Mesoderm in Xenopus laevis*. PhD Thesis, University of California, Berkeley.
- Wilson, P., Keller, R., 1991. Cell rearrangement during gastrulation of *Xenopus*: direct observation of cultured explants. *Development* 112, 289–300.
- Wilson, P.A., Oster, G., Keller, R., 1989. Cell rearrangement and segmentation in *Xenopus*: direct observation of cultured explants. *Development* 105, 155–166.
- Youn, B.W., Malacinski, G., 1981. Somitogenesis in the amphibian *Xenopus laevis*: scanning electron microscopic analysis of intrasomitic cellular arrangements during somite rotation. *J. Embryol. Exp. Morphol.* 64, 23–46.